Lead Sorption Efficiencies of Natural and Synthetic Mn and Fe-oxides

Susan Erin O'Reilly

Dissertation submitted to the faculty of the Virginia Polytechnic Institute and State University in partial fulfillment of the requirements for the degree of

Doctor of Philosophy
in
Geological Sciences

Michael F. Hochella, Jr., Chair
David F. Cox
Matthew J. Eick
J. Donald Rimstidt
Lucian W. Zelazny

September 27, 2002
Blacksburg, VA

Keywords: Manganese oxide, iron oxide, lead, sorption, microscopy, spectroscopy

Lead Sorption Efficiencies of Natural and Synthetic Mn and Fe-oxides

S.E. O'Reilly

ABSTRACT

Lead sorption efficiencies (sorption per surface area) were measured for a number of natural and synthetic Mn and Fe-oxides using a flow through reactor. The Mn-oxide phases examined included synthetic birnessite, natural and synthetic cryptomelane, and natural and synthetic pyrolusite; the Fe-oxides studied were synthetic akaganeite, synthetic ferrihydrite, natural and synthetic goethite, and natural and synthetic hematite. The sorption flow study experiments were conducted with 10 ppm Pb with an ionic strength of either 0.01 M $NaNO_3$ or 0.01 M KNO_3 both at pH 5.5. The experimental effluent solution was analyzed using aqueous spectroscopic methods and the reacted solids were analyzed using microscopy (field emission scanning electron microscopy, FE-SEM), structure analysis (powder X-ray diffraction, XRD), bulk chemical spectroscopy (energy dispersive spectroscopy, EDS), and surface sensitive spectroscopy (X-ray photoelectron spectroscopy, XPS). Overall, the synthetic Mn-oxides did have higher sorption efficiencies than the natural Mn-oxides, which in turn were higher than the natural and synthetic Fe-oxides. Only natural pyrolusite had a sorption efficiency as low as the Fe-oxides. Most of the natural and synthetic Fe-oxides examined in this study removed about the same amount of Pb from solution once normalized to surface area, although synthetic akaganeite and hematite were significantly less reactive than the rest. The observed efficiency of Mn-oxides for Pb sorption is directly related to internal reactive sites in the structures that contain them (birnessite and cryptomelane, in the case of this study). Comparisons of solution data to XPS data indicated that Pb went into the interlayer of the birnessite, which was supported by XRD; similarly some Pb may go into the tunnels of the cryptomelane structure. Layer structures such as birnessite have the highest Pb sorption efficiency, while the 2 x 2 tunnel structure of cryptomelane has lower efficiencies than birnessite, but higher efficiencies than other Mn- or Fe-oxide structures without internal reactive sites.

ACKNOWLEDGEMENTS

The author would like to thank the National Science Foundation for their generous support. I would also like to thank the National Museum of Natural History (NMNH) of the Smithsonian Institute, the Virginia Polytechnic Institute (VPI) museum, L. McKinney, and J. D. Rimstidt for their generous donations of mineral samples.

I would like to thank the Department of Geological Sciences at Virginia Tech for providing a positive and nurturing environment for graduate students. Additionally, I would like to thank my fellow graduate students. Their camaraderie made "the hard times" a little bit easier. I especially owe thanks to the past and present graduate students in my research group; they provided academic and non-academic support that I will always value. I always appreciated my "academic family", and I will miss them greatly. I hope to see you all at conferences in the future.

I also need to thank my committee for their generosity with their time, expertise, and recommendations, and often even lab equipment. The range of perspectives of my committee members has helped make this project well balanced. I especially have to thank J. Don Rimstidt and Matt Eick for all the extra help.

My advisor, Michael Hochella, deserves special thanks. He took me in, helped me develop a project, and helped me bring it to fruition despite many challenges, academic or otherwise, along the way. Without him, I would not have had the opportunity to earn my degree with so much freedom.

I am very fortunate to owe thanks to many friends, teachers, and colleagues over the years who helped shape me into the scientist and student of life that I am today. I would like to especially thank long-time friends Christi Thomas and Wendy Chou. My appreciation also goes out to past advisors J. Thomas Sims and Donald L. Sparks and his research group at the University of Delaware.

Most importantly, I thank my family. They provide an infinite source of love, support, and inspiration. I wish my grandparents James and Ethel O'Reilly and Joseph and Susan Cava were here to share this with me. I will always be grateful that "Nanny" O'Reilly got to see me make it most of the way through. I thank my sisters Katie and Kerry O'Reilly and my parents John and Susan O'Reilly for helping through this experience and understanding how important it was to me.

DEDICATION

For my parents
John T. and Susan K. O'Reilly
Who always sacrificed so that my sisters and I could have the very best of everything.

TABLE OF CONTENTS

ABSTRACT ii
ACKNOWLEDGEMENTS iii
DEDICATION iv
LIST OF TABLES vi
LIST OF FIGURES vii
1 Introduction 1
2 Materials and Methods 4
2.1 Reagents 4
2.2 Minerals 4
2.2.1 Synthetics 4
2.2.2 Natural Solids 5
2.3 Techniques 6
2.3.1 Surface area analysis 6
2.3.2 X-ray diffraction, XRD 6
2.3.3 Atomic absorption spectroscopy (AA) 6
2.3.4 Inductively coupled plasma atomic emission spectrometry (ICP-AES) 6
2.3.5 Field Emission Scanning Electron Microscopy (FE-SEM) and energy dispersive spectroscopy (EDS) 7
2.3.6 X-ray photoelectron spectroscopy (XPS) 7
2.3.7 Zeta Potential 7
2.4 Flow through Experimental System 8
2.4.1 Choice of Membrane Filter Papers 9
2.5 Data Analysis and Errors 9
3 Results and Discussion 9
3.1 IEP 9
3.2 Blanks 11
3.3 Mn Release 12
3.4 pH 12
3.5 Lead Sorption on Manganese and Iron Oxides 12
3.6 FE-SEM 13
3.7 EDS 14
3.8 XPS 14
3.9 XRD 14
3.10 Reactions in Interlayers and Tunnel Structures 15
4 Conclusions 16
5 References 18
6 Tables 23
7 Figures 27
8 Vita 43

LIST OF TABLES

Table 1. Summary of chemical and structural properties of the Mn and Fe-oxides used in this study. .. 23
Table 2. Estimated Isoelectric Points, IEP, of the Mn and Fe-oxy(hydr)oxides used in this study. 25
Table 3. Comparison of Pb sorption data from flow study to XPS data in the $NaNO_3$ background electrolyte..... 26

LIST OF FIGURES

Fig. 1. Lead sorption to Mn and Fe-oxides in terms of surface area of the solid. 27
Fig. 2. Schematic of sorption flow study showing the components of the experiment and the direction of flow. 28
Fig. 3. Lead solubility diagram showing pH and Pb concentration at which the lead solids massicot and hydrocerrusite form at atmospheric carbonate levels. 29
Fig. 4. "Blank" flow system experiments in KNO_3 background electrolyte 30
Fig. 5. Lead sorbed in the NaNO3 matrix without any solid, mineral-blank in $NaNO_3$, versus pH. 31
Fig. 6.. Blank experiment without Pb or mineral solid in KNO_3 electrolyte, mineral – Pb-blank in KNO_3. 32
Fig. 7. Lead sorbed on synthetic cryptomelane in $NanO_3$ background electrolyte and reaction pH. 33
Fig. 8. Total Pb sorption on Mn-oxides displayed normalized to the BET surface area of the respective solid. 34
Fig. 9. Total Pb sorbed on Fe-oxides displayed normalized to the BET surface area of the respective solid. 35
Fig. 10. Total average Pb sorption in $\mu mol/m^2$ after approximately 118mL of solution has passed through each reactor. 36
Fig. 11. FE-SEM image of synthetic birnessite. 37
Fig. 12. FE-SEM image of synthetic cryptomelane. 38
Fig. 13. FE-SEM image of natural cryptomelane, Cr1. 39
Fig. 14. FE-SEM image of natural cryptomelane, Cr2. 40
Fig. 15. EDS spectra of natural cryptomelane, Cr1. 41
Fig. 16. XPS survey scans of unreacted synthetic birnessite in KNO_3 and selected Pb reacted samples in $NaNO_3$ background electrolyte. 42

1 INTRODUCTION

Manganese oxides are typically thought to be the most important scavengers of aqueous trace metals in soils, sediments, and rocks through their seemingly dominant sorptive behavior despite the fact that they are much less abundant than iron oxides (e.g. Burns, 1976; Chao and Theobald, 1976; Jenne, 1968; Schwertmann and Taylor, 1989). In both the cases of Mn and Fe-oxides, their reactivity and generally high surface areas make them proficient sorbents of many inorganic cations such as Cu, Pb, Zn, Co, and Ni, among others (e.g. Jenne, 1968; McKenzie, 1980; Schwertmann and Taylor, 1989; McBride, 1994). In particular, manganese (III/IV) and iron (III) oxide/hydroxide mineral particles and coatings in soils seem to have a strong affinity for Pb (Rickard, 1978), and soils represent the major near surface sink for anthropogenic sources of this metal (Nriagu, 1978). Thus these minerals may be able to effectively sequester Pb, one of the most common (Nriagu, 1978) and extensively distributed toxic metals in the environment (Boeckx, 1986; Kaim, 1994).

Research has shown that Pb collects in soil Mn-oxides (Norrish, 1975), and when Mn-oxide was added to Pb contaminated soils, Pb uptake by plants was reduced (McKenzie, 1978). Several studies have also shown that Pb sorption was greater than for other metals, including Ba, Cd, Co, Cu, Mn, Ni, and Zn on various Mn-oxides (Aualiitia and Pickering, 1987; Gadde and Laitinen, 1974; McKenzie, 1980; Parida et al., 1996; Van der Weijden and Kruissink, 1977). Additionally, other studies have indicated that Mn-oxides generally sorbed more Pb than other phases such as Fe-oxides, Al-oxides, organics or clays (Aualiitia and Pickering, 1987; Dong et al., 2000; Gadde and Laitinen, 1974; McKenzie, 1980). Hudson-Edwards (2000) also found that Mn-oxides in sediments did contain considerably more Pb than Fe-oxides. Finally and not surprisingly, it is common for authors, in reviewing the literature, to state that Pb is preferentially accumulated by Mn-oxides (e.g. Nriagu, 1978; Balistrieri and Murray, 1986; Paulson et al., 1988; Manceau et al., 1992; Dahal and Lawrance, 1996; Morin et al., 1999).

Unfortunately, some of this information reviewed above seems to have been misleadingly propagated though the literature. When discussing Pb uptake, many papers cite the excellent review by Jenne (1968). However, this study did not investigate the role of hydrous Mn and Fe oxides on Pb concentrations in soils and waters, but instead Mn, Fe, Co, Ni, Cu, and Zn. Further, Taylor and McKenzie (1966) concluded from soil extraction studies that, even though Co, Ni, Mo, Ba, Zn, V, Cr, and Pb tend to be more concentrated in manganese minerals than whole soils, only Co seemed to have a significant, specific affinity for the Mn-oxide fraction of the soil. The authors did not find a linear correlation between the Pb content and the soil Mn fractions. Kabata-Pendias (1980) found that Pb was “fixed” by Mn-oxides along with Zn and Cd, but Pb was also easily “fixed” by Fe-oxides. A study by Ostergren et al., (1999) discovered that in natural, contaminated samples Fe-oxides play a much more substantial role in the adsorption of Pb than Mn-oxides do.

Other studies also failed to find a correlation between Pb and Mn-oxides. Li (1982) conducted enrichment calculations on elements of manganese nodules and related sediments and concluded that Pb is concentrated in the Fe-oxides, not the Mn-oxides in the nodules. A study by (Carpenter et al. (1975) evaluated the concentration of certain metals in the black coatings on stream boulders and showed that the coatings effectively reflected Zn and Cu mineralization in drainage basins, but not Pb. Lead was not concentrated in the coatings. Dong et al. (2001) also noted that there are different views on the importance of Mn, Fe-oxides, and even organic matter.

Clearly there are discrepancies as to whether Mn-oxides are particularly efficient at sorbing Pb, and beyond that, if they are more efficient at sequestering Pb than Fe-oxides.

We have only found one paper by McKenzie (1980) that examined both the sorption of Pb on multiple Mn-oxides in comparison to Fe-oxides and, for a portion of the study, looked at the Pb uptake of these solids normalized to their surface area. All of this work was done in batch reactors. In Fig. 1., which was adapted from McKenzie (1980), we show the sorption of the various solids normalized to surface area. McKenzie's data shows that the synthetic Mn-oxides sorb an order of magnitude more Pb per surface area than the Fe-oxides, in some cases dramatically so (Fig. 1). The amount of Pb sorbed was, however, greatly affected by the synthesis method of the solid.

Three Mn-oxides had particularly high sorption affinities in the McKenzie (1980) study. Those solids were two of the many synthetic birnessites studied and one of the cryptomelane samples. No evidence was found for the oxidation of Pb(II) to Pb(IV) nor for the formation of new solid phases. X-ray diffraction studies provided some evidence that Pb went into the interlayer of birnessite, which explained the high sorption capacity, exhibited by some of the birnessite samples. However, the cause of the higher sorption capacity of the one cryptomelane was unclear. Interestingly in Fig. 1, those same three solids no longer seem to have such extraordinary sorption capacities. As seen in Fig. 1, one birnessite does have an extraordinary sorption capacity, and several birnessite and cryptomelane samples have high sorption capacities with the remainder of the samples all sorbing fairly similar amounts. So, once normalized to surface area, the drastic sorption of the cryptomelane sample shown in the original McKenzie (1980) plot is no longer so difficult to explain.

The types of studies that exist correlating Pb to Mn-oxides in soils fall into three categories: (1) extraction or selective extraction studies, (2) microprobe studies, and (3) sorption studies. All these studies have increased our knowledge of these systems. However, extraction studies are plagued with artifacts such as removal of both Mn and Fe oxides and redistribution of Pb species among soil mineral phases (Chao and Theobald, 1976; Gilmore, 2001; McCarty et al., 1998; Ostergren et al., 1999; Taylor and R.M., 1966). Microprobe techniques are not surface sensitive and can be restricted by their detection limits for trace elements such as Pb (see Goldstein et al., 1992; Ostergren et al., 1999; Rauch et al., 2000). Sorption studies are often much more controlled than the extraction or microprobe studies because pure Mn-oxides are specifically synthesized for these studies. However, these synthetic phases have not been compared to natural phases to see how good of a proxy they are for the environment. The sorption studies rarely compare multiple synthetic Mn-oxide phases to the "same" minerals collected in nature or to other solids such as Fe-oxides. Even fewer of these studies normalize their data to the surface area of the solids mentioned, and this may be the cause of some of the contradictions in the literature.

Thus, the goals of our study are to (1) thoroughly examine the Pb sorption efficiency (i.e. amount sorbed per surface area) of several synthetic and natural Mn and Fe-oxides using well-characterized samples and flow-through reactor techniques, (2) obtain insight into what factors determine Pb sorption efficiency, and (3) clarify as many ambiguities or misconceptions in the existing literature as possible. Our study has the distinct advantage of having access to a suite of well-characterized, natural Mn-oxides along with a variety of synthetic Mn-oxides. Also, by taking into account surface area and performing flow through experiments, we avoid many of the inherent problems in previous studies.

Lead sorption studies were conducted using a flow through reactor so that chemical steady state conditions were maintained during the experiments (Rimstidt and Newcomb, 1993; Sparks, 1995). The experimental design also had in-line pH monitoring capabilities so that hydrogen evolution could be monitored. Figure 2 shows a schematic of the experimental design and conditions. The experiments were conducted with 10 mg/L Pb (48.3 μM) with an ionic strength of 0.01 M in $NaNO_3$ at pH 5.5 and also with 0.01 M KNO_3 with all other conditions being the same. Under these conditions, the experiments were undersaturated with respect to all known lead hydroxides and carbonates (see Fig. 3; an asterisk denotes the conditions of this study on the solubility plot). The experimental effluent solution was analyzed using aqueous spectroscopic methods and the reacted solids were analyzed using microscopy (field emission scanning electron microscopy, FE-SEM), bulk surface chemical spectroscopy (energy dispersive spectroscopy, EDS), and surface sensitive spectroscopy (X-ray photoelectron spectroscopy).

This Pb concentration was chosen to (1) allow for the oxides to sorb significant amounts of Pb, (2) limit any analytical difficulties and errors that arise when working with very low concentrations near detection limits, and (3) to reflect the Pb exposure of soil minerals at highly contaminated sites. Extremely wide ranges are reported for the Pb content values for both uncontaminated and contaminated soils (see Chlopecka and Adriano, 1997; Davies, 1995), and soil solution values are rarely reported. Tampouris et al. (2001) studied an acidic (pH 5.6, similar to this study) soil that was contaminated from mining activities with approximately 16,000 mg Pb/kg dry soil. Gregson and Alloway, (1984) extracted the soil solution from several contaminated soils and found soil solution values ranged from 4 mg/L to 112 mg/L.

The Mn-oxides we studied are birnessite, pyrolusite, and cryptomelane. Birnessite ($K_4Mn_{14}O_{27}\bullet 9H_2O$, adapted for the potassium from Burns, 1976 or $(Na,Ca,Mn^{2+})Mn_7O_{14}\bullet 2.8\ H_2O$ Post, 1992) is also occasionally referred to as manganous-manganite or δ-MnO_2 (e.g. Frondel et al., 1960; McKenzie, 1971), but many more recent studies refer to δ-MnO_2 as vernadite (a disordered birnessite only exhibiting two X-ray diffraction lines) (see Burns, 1976; Giovanoli, 1980; McKenzie, 1989; Post, 1992; Yang and Wang, 2002). Birnessite is the most common Mn oxide in soils and is generally found as discrete soil nodules, dessert varnishes, and ocean nodules (Burns and Burns, 1979; Dixon and Skinner, 1992; McKenzie, 1989; Post, 1992; Taylor et al., 1964). All known natural birnessite samples are either poorly crystalline or consist of minute crystals; thus these materials have not been extensively characterized (Post, 1992). Birnessite does have a layer structure with both Mn^{3+} and Mn^{4+} (Post, 1992). Pyrolusite (β-MnO_2) is the most stable form of MnO_2, but it is rare in soils because even small amounts of foreign ions prevent the formation of pyrolusite (McKenzie, 1989). It is generally found in low temperature hydrothermal deposits and as alteration products of other Mn-oxide minerals (Post, 1992). Pyrolusite is a framework structure containing tunnels (1 X 1 octahedra) formed by edge-linked $Mn(IV)O_6$ octahedra sharing corners with neighboring chains (Post, 1992). Cryptomelane ($K_x(Mn^{4+}Mn^{3+})_8O_{16}$($x\approx 1.3$-1.5) or generally α-$MnO_2$) is part of the hollandite group (McKenzie, 1989; Post, 1992), and its structure consists of double chains of edge-sharing Mn-O octahedra that share corners with each other to form a framework structure with 2 X 2 (octahedral on edge) tunnels (Post, 1992). The tunnels are partially filled with large mono or divalent cations and sometimes water molecules (Post, 1992). The charges on the tunnel cations are balanced by substitution of Mn^{2+} or Mn^{3+} on the octahedral site (Post, 1992). The minerals within the hollandite group are defined on the basis of the principal type of tunnel cations as follows: hollandite (Ba), coronadite (Pb), and cryptomelane (K) (McKenzie, 1989; Post, 1992). McKenzie (1989) describes this group of minerals as “reasonably common” in soils. The

hollandite group occurs in a variety of environments such as oxidized areas of Mn deposits and sedimentary deposits (Hewett and Fleischer, 1960). Large crystals of hollandite and cryptomelane have been a rare find in hydrothermal veins (Post, 1992).

Iron oxides were also tested in this study because Pb sorption is often attributed to Fe-oxides in soils as well as or rather than Mn-oxides. The Fe-oxides listed below have been chosen because they are either very common phases in nature or they are isostructural with one of the Mn-oxide phases we planed to study. Goethite (α-FeOOH) is the most common and thermodynamically stable iron oxide in soils. Goethite has double rows of $FeO_3(OH)_3$ octahedra, which share edges and corners to form 2 X 1 octahedra "tunnels" (only large enough to accommodate the passage of protons) partially bonded by hydrogen bonds (Schwertmann and Cornell, 1991; Sparks, 1995; Cornell and Schwertmann, 1996). Hematite is the second most common iron oxide in soils (Sparks, 1995). Hematite (α-Fe_2O_3) consists of FeO_6 octahedra connected by edge- and face-sharing (which causes distortion in the cation sublattice from ideal packing) (Sparks, 1995; Cornell and Schwertmann, 1996). Ferrihydrite is a poorly ordered Fe^{3+} oxide that has short range ordering and is prevalent in surface environments where it is often a precursor for other Fe-oxides (Schwertmann and Taylor, 1989; Cornell and Schwertmann, 1996). Akaganéite (β-FeOOH) is isostructural with cryptomelane (Cornell and Schwertmann, 1996).

2 MATERIALS AND METHODS

2.1 Reagents

All chemicals used in the experiments were reagent grade or better. Trace metal grade or standardized acids and bases were used for pH adjustments. High-purity distilled, deionized water from a Millipore Synthesis A10 water system (18.2 MΩ, <8ppb total organic carbon (TOC), UV light treated, ultrafiltration membrane, 0.2 μm filtered) was used to make all solutions. All glass and plastic ware was acid washed using a 0.1 N nitric acid bath; if any dishes appeared to be stained by Mn or Fe oxides, they were soaked in a 0.1 N oxalic acid bath. The dishes were then soaked in distilled, deionized water.

2.2 Minerals

Both natural and synthetic Mn and Fe-oxide mineral samples were used in this study. For convenience, we have used the corresponding mineral name even for the synthetically prepared oxides (e.g. synthetic cryptomelane instead of α-MnO_2). The identities of the solids were verified using X-ray powder diffraction. The samples were further characterized by low-voltage field-emission scanning electron microscopy (FE-SEM), energy dispersive spectroscopy (EDS), BET N_2 adsorption surface area, and isoelectric point (IEP) measurements.

2.2.1 Synthetics

Synthetic Mn-oxides were made using recipes found in McKenzie (1971). When necessary, the "recipes" were scaled back (i.e. less sample was prepared) for ease of preparation in our laboratory. Unless otherwise noted, all the solids were washed with trace metal clean dialysis tubing (Fisherbrand, 32mm, 10,000 MWCO) until the conductivity of the soaking water matched that of distilled, deionized water; once washed, the samples were freeze dried.

Synthetic K-birnessite was prepared by reducing a potassium permanganate solution by boiling the solution during dropwise addition of HCl. After cooling enough to handle, the precipitate was separated by filtration and rinsed before dialyzing. Synthetic cryptomelane (α-MnO_2) was prepared by converting birnessite (prepared as noted except rinsed and air-dried rather than dialyzed and freeze-dried) to cryptomelane by ignition at 400 °C for 60 hours.

Synthetic pyrolusite (β- MnO_2) was prepared by ignition after evaporation of manganous nitrate. Certified manganese(ous) nitrate 50% solution was poured into an evaporating dish and placed under a hood to evaporate. After 1 day, a 100 W heat lamp was placed 15 cm above the evaporating dish. After 6 more days, the sample was not fully evaporated but had changed color so it was placed in an oven at 180 °C for 48 h. The sample was ground in a mortar and pestle, washed with dialysis tubing, and returned to the oven for 24 h. This sample was not freeze-dried since it was washed prior to being put back in the oven. The edges of the evaporating dish had a shiny, metallic precipitate whereas the bulk of the precipitate was course textured and dull gray in color. The precipitates were separated by hand and the dull, gray precipitate was used in the experiments. Initial FE-SEM and EDS analysis of the pyrolusite showed a salt coating was still on the precipitate so the sample was washed again by rinsing and centrifuging multiple times and then dried at room temperature before use in the experiments.

Synthetic Fe-oxides were made according to the methods of Schwertmann and Cornell (1991). The precipitates were dialyzed and freeze-dried analogous to the Mn-oxides. Synthetic akaganeite was prepared by hydrolysis of acidic $FeCl_3$ solutions by preparing a 0.1 M solution of $FeCl_3$ in a closed flask at 40 °C for 8 d. The recipe calls for 2 L of solution to be stored in a closed 3 L flask (Schwertmann and Cornell, 1991), but our solution was split into four, 1 L high-density polyethylene bottles in order to fit into our oven. After 3 d, no precipitate was forming so the temperature was raised to 70 °C because the authors noted that this might increase the yield of the solid. Schwertmann and Cornell (1991) do describe an alternate method using NaOH that also uses 70 °C temperatures. The supernatant was siphoned off and the precipitate was further separated by centrifugation before being washed. Hematite was synthesized using "method 1" of Schwertmann and Cornell (1991) which involves the forced hydrolysis of a Fe(III) salt solution. The preparation was split into two, 1 L bottles consisting of 0.002 M HNO_3 that were heated to 98 °C in an oven. The bottles were removed from the oven and 8.3 g of $Fe(NO_3)_3 \cdot H_2O$ was added to each of them while stirring. The bottles were then sealed and returned to the oven for 7 d. The samples were allowed to cool before handling, some of the supernatant was poured off, and then the samples were centrifuged before being washed. Six-line ferrihydrite was synthesized by hydrolysis of an acidic Fe(III) solution (Schwertmann and Cornell, 1991). Two liters of distilled, deionized water were heated to 75 °C in an oven prior to adding 20 g of $Fe(NO_3)_3 * 9H_2O$ while stirring. The solution was returned to the oven for 12 more minutes and immediately placed into an ice water bath. The solution was then put into a 4 °C refrigerator in between being prepped for dialysis.

2.2.2 Natural Solids

Table 1 lists the natural solids used in this study, the lending party, the original sample location if known, and the JCPDS card file or reference used to confirm the identity of the solids. The natural solids either were obtained from the National Museum of Natural History (NMNH) of the Smithsonian Institution, the Virginia Polytechnic Institute (VPI) museum, or generously donated by private collectors. Since synthesizing solids yields a fine-grained mineral form suited toward our flow experiments (also a grain size often found in soils and sediments), most of the natural solids needed to be reduced in size. Large mineral fragments were crushed to < 0.5 mm in a percussion mortar and then were wet-ground in distilled, deionized water for 10 minutes using a McCrone Micronizing Mill (a vibrating rod mill). This method is the best way of reducing particle size while avoiding many of the negative effects associated with more aggressive, traditional grinding methods (Buhrke et al., 1998).

2.3 Techniques

2.3.1 Surface area analysis

Surface area was measured using the BET N_2 adsorption method using a Nova 1200 high-speed surface area and pore analyzer manufactured by Quantachrome. Single and 5-point BET measurements were made. Sorption data is normalized according to the 5-point measurement, but the two measurements agreed well. Samples were vacuum degassed overnight at 40 °C to minimize the possibility of phase changes during high temperature degassing.

2.3.2 X-ray diffraction, XRD

XRD was used to identify the natural and synthesized solids. Powder measurements were taken using a Scintag XDS 2000 X-ray powder diffractometer. Powder mounts were prepared directly in the sample holders or on zero background plates depending on the amount of sample. A CuKα radiation source was used and the window on the detector was adjusted to minimize the contributions of fluorescence. Continuous scans of reacted solids on filter paper and synthetic birnessite were run from 4 to 70 degrees 2θ. Reacted solids were scanned at 4°/min; because of the poorly crystalline nature of birnessite, it was scanned at 1°/min. All other scans were made from 10 or 20 (depending on expected peaks and background) to 70 degrees 2θ at a scan rate of 4°/min. The samples were spun in order to minimize the possibility of any preferential orientation in the mounts.

2.3.3 Atomic absorption spectroscopy (AA)

Analysis of aqueous Pb was performed using a Buck Scientific 200-A AA. Four standard dilutions of a purchased 1000 ppm Pb AA standard reference solution (Fisher chemical) ranging from 0.8 to 12 ppm Pb were analyzed to produce a calibration curve of absorbance versus concentration. The standards were made in the identical matrix used in each of the runs. The standards were measured in triplicate at the beginning and end of each run; average values were used to plot the calibration curve. The AA was adjusted to a slitwidth of 7Å, a wavelength of approximately 283.3 nm, and a 5.0 mA lamp current using an air-acetylene flame. The sensitivity for this method is reported as being approximately 0.2 mg/L (ppm) (Welz and Sperling, 1999). All the measurements were taken in triplicate and averaged before being converted to concentration. The AA was operated on integration mode to eliminate the measure of errors due to random noise; this method averages the signal taken over 7 seconds before reporting a reading (Buck Scientific, 1992). The AA was rinsed and rezeroed between every sample to avoid contamination and drift.

2.3.4 Inductively coupled plasma atomic emission spectrometry (ICP-AES)

Analysis of KNO_3 matrix samples for Pb and Mn or Fe (for Mn and Fe-solids respectively) was performed on a Spectro Analytical Instruments SpectroFlame (type FTMA85D) ICP. The ICP was used because of its low detection limits for Mn and its ability to measure multiple elements at once. The measurements were performed at wavelengths of 168.220 nm for Pb, 257.610 nm for Mn, and 259.940 nm for Fe. Measurements were taken from the sample in triplicate. Lead analysis on the ICP was found to correspond well with AA analysis of Pb for the

same samples. The ICP generally detects Pb in the analytical range of 0.05-10,000 ppm, Mn from 0.001-5000 ppm, and Fe from 0.002-10000 ppm.

2.3.5 Field Emission Scanning Electron Microscopy (FE-SEM) and energy dispersive spectroscopy (EDS)

Low voltage FE-SEM imaging and EDS analyses were performed with a LEO 1550 FE-SEM with Kevex EDS detector. Some unreacted Mn-oxides and many of the Fe-oxides (especially less crystalline samples) were conductively coated for ease in imaging; however, many samples were not coated at all. Experience in our laboratory has shown that when operating the FE-SEM at low voltage (<5 kV) and using the "SE^I" detector, excellent lateral resolution of <5nm can be achieved (Weaver, 2001). The backscatter detector was also used to check for Pb precipitates on the surfaces of the oxides. The beam was often adjusted in one area, moved, and then an image was quickly taken to avoid beam damage to any possible precipitates. EDS analysis was taken at lower magnifications and higher voltages (≈20 kV).

2.3.6 X-ray photoelectron spectroscopy (XPS)

Selected samples were analyzed with a Perkin-Elmer 5400 using an Al X-ray source. Survey spectra of selected solids were collected with a pass energy of 44.75 eV from 0-1000 eV binding energies for 5 minutes. High-energy resolution scans of Mn2*p* and Pb4*f* peaks were collected from 630-670 and 130-150 eV binding energies, respectively using a pass energy of 17.90 eV. The Pb/Mn atomic ration was calculated using standard sensitivity factors obtained from standards measured in the 5400 hemispherical electron energy analyzer. The analysis area of each sample was approximately 1 x 3 mm.

2.3.7 Zeta Potential

A Malvern Instruments ZetaSizer 3000 HSa was used to measure the electrophoretic mobility via laser Doppler velocimetry. Mixed Mode Measurements were used in order to minimize the deleterious effects of electrosmosis. The zetasizer estimates the zeta potential from the electrophoretic mobility using the Smolouchowski equation. The isoelectric point (IEP), the point at which the electrokinetic potential equals zero (Kosmulski, 2001), was determined by plotting the average of at least three zeta potential measurements each at a minimum of six different pH values for solids that were hydrated in the background matrix (0.01 M $NaNO_3$ or 0.01 M KNO_3) for at least 4 days and then pH adjusted over at least 6 days. The suspension density used in the experiments was 0.25 mg/L (except for the ferrihydrite which was run at 0.125 mg/L) and the samples were sonified to encourage dispersion. The pH was adjusted in a series of centrifuge tubes filled with 25 mL of suspension by microliter additions of 0.1 M HNO_3 and 0.1 M NaOH or KOH (corresponding to $NaNO_3$ and KNO_3 matrices respectively). The final pH was measured at the same time that an aliquot of the suspension was being analyzed in the zetasizer. The zeta potential values were plotted against pH and the IEP pH value was determined from the intersection of the data with the zero potential axes. Since the exact shape of the plot cannot be predicted, this method does not allow for extrapolation; thus, solids with a very low IEP such as birnessite can only be estimated to be below a certain pH; for a true IEP value, points need to be collected at positive and negative potentials.

2.4 Flow through Experimental System

Lead sorption studies were conducted using a flow through reactor so that chemical steady state conditions were maintained during the experiments (Rimstidt and Newcomb, 1993; Sparks, 1995). A schematic of the flow reactor along with key experimental parameters are illustrated in Fig. 3. The experiments were initially run in duplicate; after acquiring a third pump, all the experiments were run in triplicate. The influent Pb concentration was 10 ppm (48.3 μM) adjusted to an ionic strength of 0.01 M with $NaNO_3$ for one set of experiments and KNO_3 for another set of experiments. The pH of the influent solution was pre-adjusted to pH 5.5; under these conditions, as shown in Fig.2, the system was undersaturated with respect to known lead oxides and hydroxy carbonates. Tygon tubing was used everywhere except for the tubing link that is inserted in the pressure plate of the cassette pump. The tubing link was made of Manostat Manosil tubing with cuffs to ensure uniform placement and tension in the pumps. The pumps were Manostat Junior or Jimmy cassette pumps (model 42-510-000). To minimize flow variations, a brand new tubing link was used for every experiment. Since Pb is known to sorb onto the walls of containers, each link was pretreated with influent Pb solution (pH and ionic strength adjusted) for at least 4 hours and then rinsed with matrix solution before its use. The influent bottles and Tygon tubing were reused for each experiment, but the system was flushed with the new matrix solution before starting runs in the new matrix.

The reactors consisted of 25 mm Swin-Lok polycarbonate filter holders (Corning) with the sorbent wet packed onto a 0.2 μ Pall Gelman Supor membrane filter paper (see next section for choice of filters). All of the solids in powder form were pre-hydrated in the appropriate matrix solution overnight, sonified, and adjusted to pH 5.5 over a minimum of 5 days before being loaded onto the reactor. The filter paper was placed into the reactor (filter holder) and rinsed two times with 2 mL of pH-adjusted matrix solution by pipetting the solution into the barrel of a syringe attached to the filter holder on a vacuum flask that was connected to an aspirator run at ≤ 5 kPa. Then the reactor was wet loaded with the appropriate amount of the solid suspension to yield 0.5 m^2 surface area of solid except for synthetic pyrolusite, which was run at 0.06 m^2 due to its very low surface area. The solid suspension was rinsed into the reactor three times with 2 mL of pH-adjusted matrix solution. In-line pH measurements were made using a pH cell made of polycarbonate holding an Accumet (model 13-620-181) rugged bulb pH electrode. The pH electrode was wired to a Prober pH 8 datalogger (Erhlich Industrial Development Corporation, E.I.D.) and connected to a computer, which recorded pH readings every two minutes.

Samples were collected by fraction collectors every 20 minutes into tubes that were previously acid washed, soaked in distilled, deionized water, and pre-acidified with trace metal grade HNO_3. The tubes were weighed and labeled before the start of the experiment and then were reweighed at the end of the experiment to more accurately determine the total amount of solution passed through the reactors and to closely monitor the flow rates. The collected fluid samples were refrigerated until analyzed by AA or ICP.

Experiments were deemed acceptable if the flow rate was >0.40 or <0.75 mL/min; the average flow rate was 0.55 mL/min. Within this flow range, flow rate did not correlate to Pb sorption. Runs with flow rates higher than 0.75 mL/min did occasionally show correlation of Pb sorption amounts with flow rate, this probably due to channelized flow in the packed reactors. The results of these runs were not used. Other runs were eliminated due to leaks in the system or other mechanical problems. Different types of "blank" experiments were run to better understand our system. A set of "blank" experiments was conducted (1) without mineral solid (2) without Pb influent solution or mineral solid, and (3) without Pb influent solution. The set of

"blanks" run without Pb influent solution were run only with the cryptomelane mineral solid in KNO_3 to determine the cause of Mn release from the cryptomelane samples. All "blank" samples were run through the same physical apparatus as shown in Fig. 3 including filter paper and the appropriate, pH adjusted background electrolyte.

2.4.1 Choice of Membrane Filter Papers

The Pall Gelman Supor membrane filter paper, a polyethersulfone membrane, was chosen after testing several filter papers of varying composition and brands for Pb sorption. While developing our experimental methodology, it was discovered that Pb was being sorbed by the MCE membranes (comprised of a mixture of cellulose acetate and cellulose nitrate) that had been used initially. Teflon and polycarbonate filter papers were two other compositions that were tested. The hydrophobic nature of Teflon filters makes them more difficult to work with in these types of experiments. However, suitable results were also found with polycarbonate filter papers. The Supor filter papers were ultimately chosen after discussions with the company regarding manufacturing processes; we were also concerned about the filters introducing metals into our experiments. Of course, there will be variability from one filter to the next as well as one lot to the next. Jardine et al. (1986) examined similar concerns with filter papers in experiments involving aqueous aluminum and similarly found that many types of filter papers released hydrogen ions to solution and/or removed Al from solution. The authors concluded that polycarbonate filters were best for their study, but washed polysulfone membranes worked as well; polyethersulfone membranes, the type used in this study, were not tested. Specific experimental results obtained from the filters we used are given in the Results and Discussion section below.

2.5 Data Analysis and Errors

A sample of the influent solution was collected from the flow lines before it entered the reactor and measured by AA or ICP using the same protocol as for the reactor output described above. The amount of Pb sorbed onto the sample was determined by difference. The amount of Pb sorption was normalized to the BET surface area of the solids to give units of μmol of Pb sorbed per m^2 of solid. Since some studies had higher flow rates than others, we did not want to compare the amount of Pb sorbed after 5 hours (the end of the experiment); instead we decided to pick the highest reasonable volume of solution that passed through all the reactors. Therefore, the total amount of Pb sorbed after an average of 119.8 mL of solution was passed through the reactors was used to compare the amount of Pb sorbed to the different solids (sampling was based on time (test tubes collected solution for 20 minutes), so the amount of solution passed through the samples actually ranges from 113-124 mL). Overall, this method allows for the direct comparison of the many different solids examined in this study.

The possible sources of error in our study are analysis errors (AA and ICP), variations in the filter paper sorbates and leachates, variations in flow due to the packing of the different solid particles or the pump, BET measurement errors (since used to normalize our data), possible sample heterogeneity, and possible differences in the surface area of the aliquot of sample used in the reactor versus that measured in the BET.

3 RESULTS AND DISCUSSION

3.1 IEP

IEP estimates for the solids examined in this study are shown in Table 2. Where extrapolation would be needed due to the nature of the sample, or due to the limited pH range of

some of the samples, greater than or less than symbols are used to indicate the approximate IEP value. As can be found in the literature, the IEP values (as well as point of zero charge, pzc, and similar values) of the solids range widely. Cornell and Schwertmann (1996) and references therein (Cornell and Schwertmann, 1996) show IEP values ranging from 7.4-9.5 for goethite, 6.4-7.3 for akaganeite, and 7.0-9.4 for hematite. The authors note that the IEP is very sensitive to impurities, thus we would expect that natural samples could have very different IEP values than synthetic samples. The extensive review by Kosmulski (2001) and references therein show IEP ranges for goethite (and synthetic α-FeOOH) of approximately 5.6-9.5, hematite from 3 to 9.5, and ferrihydrite from 7.2-9.8 (see Kosmulsk, 2001 for more details and specific references). Mn-oxide IEP values also range widely; pyrolusite ranges from 4.4 to 7.3, and cryptomelane only had one IEP value reported at about 4.6, but other methods reported values ranging from 3-5.4 (Kosmulski, 2001 and references therein). Measuring the zero charge conditions of birnessite is very difficult as the values reported are generally extremely low as discussed in the methods section of this paper; most values are only obtained from methods that allow somewhat reliable extrapolation and are not actually directly measured. Healy et al. (1966) notes that potentiometric titrations are difficult because the methods require that solids have a large surface area and a zpc (zero point of charge) ranging from 3 to 11. Murray (1974) could not get IEP measurements below pH ≈2.5 because of combined effects of the reduction in surface charge and an increase in ionic strength made the δ-MnO_2 suspension unstable. Of course at low pH values, the possibility of dissolution of the solid is also a concern as noted by Murray (1974) for pH values below 3.5. McKenzie (1981) also noted that point of zero salt effect titrations were difficult at very low pH values because the titration curve became very flat and inaccurate in addition to the dissolution of the solid. Regardless, methods other than IEP determination show a range of values for the pH at zero charge conditions ranging from 1.5 to 3.6 (see Kosmulski, 2001).

The limited information on Mn-oxides in common compilations and textbooks generally report that most Mn-oxides have IEP or pzc values below that of most Fe-oxides (i.e. Langmuir, 1997; Sparks, 1995; Zelazny et al., 1996). Under the conditions of our study, Mn-oxides did generally have lower IEP values in $NaNO_3$ solutions than Fe-oxy(hydr)oxides did. However, the same observation does not hold for the values measured in KNO_3 background electrolyte solutions. Fe-oxide measurements are virtually identical in either matrix, but the IEP of the Mn-oxides in the KNO_3 matrix are most often significantly greater than in the $NaNO_3$ background electrolyte. At pH 5.5 (the pH of the sorption experiments reported in this study), Fe-oxides, with the exception of one natural hematite sample M2258, would have a net positive charge on the surface. The Mn-oxides in KNO_3 also have a net positive charge on the surface with the exception of birnessite. In $NaNO_3$, all the Mn-oxides, except the natural cryptomelane sample (Cr 2) and possibly synthetic cryptomelane, have a net negative charge. If electrostatics were to play a major role in the reaction of aqueous Pb with the oxides, then sorption on the solids would follow the order Mn-oxide > Fe-oxides in $NaNO_3$ (with noted exceptions) and Fe-oxides ≈ Mn–oxides in KNO_3. Pb sorption should be greater in the $NaNO_3$ matrix than in the KNO_3 matrix.

Interestingly, the shift in the IEP of the Mn-oxides in the presence of K versus Na may indicate that K is interacting preferentially or differently with these surfaces. Other studies have come to similar conclusions. Healy et al. (1966) found that δ-MnO_2 and α-MnO_2 (disordered birnessite or vernadite and cryptomelane, respectively) zpc values increased with increasing ionic strength above 10^{-3} M. However, β-MnO_2 and γ-MnO_2 (pyrolusite and nsutite respectively) yielded the same zpc values at ionic strengths as high as 1M $NaNO_3$. The authors

thought this process was related to ion exchange phenomena. Balistrieri and Murray (1982) noted that, at pH 8 in seawater, the association of electrolyte ions rather than the dissociation of protons would dominate the surface of δ-MnO_2. The authors concluded that the adsorption of Na, Mg, Ca, and K appear to be basically electrostatic, but suggest that the associations of Na and K are slightly stronger than simple electrostatics interactions due to the magnitude of their intrinsic equilibrium constants. The authors later go on to say that Na and K form monodentate complexes with the surface and that Ca and Mg form bidentate complexes with the surface. The adsorption of Mg and Ca ions on the surface occurred by exchange with Na and K ions as well as protons. Murray (1974) used δ-MnO_2 and assumed solely electrostatic interactions between Na and K. Sodium and K electrolyte solutions were used as sorbates to help determine the pzc of the solid; Na sorption was greater than K sorption to the surface. The pH had to be lowered more to remove the K from the surface than to remove Na. The authors concluded that the interaction of Na with MnO_2 is in response to the charged surface, which results from the dissociation of surface protons. Yousef et al., (1971) studied β-MnO_2 and found that changing the cation of the supporting electrolyte by using 10^{-3} M KNO_3 vs. $NaNO_3$ produced a slightly less negative ξ potential. This discussion bears further consideration when the sorption study results are discussed below.

3.2 Blanks

Figure 4 shows the results of the various blank runs, which were used to assess the potential uptake and release of Pb into/from the system from other components besides the mineral sample. Starting from the left, the figure shows a typical amount of Pb sorbed by the experimental system when a Pb and KNO_3 containing influent solution is passed through the system in the absence of a mineral powder. In other words, this blank experiment was run exactly as the regular experiments except that no mineral was put into the reactor. This is referred to below as a mineral- blank run in KNO_3. The next part of Fig. 4 is the average of duplicate runs of another type of blank run in the KNO_3 matrix; this run consists of only KNO_3 background electrolyte and has no Pb in solution or mineral in the reactor. It is referred to below as a mineral-Pb-blank run. The rest of Fig.4 shows the small amounts of Pb that were released from the cryptomelane solids that were run solely with the KNO_3 background electrolyte, the Pb-blank for the mineral cryptomelane in KNO_3 background electrolyte (see Fig. 4). The quantities were less than the amount of Pb released by the filter papers alone.

We chose the best filter papers available for our experiments (see Experimental section above), but obviously they are not ideal and, of course, they can be variable. In addition, trace amounts of Pb can be released. This variability along with slight fluctuations in flow rates makes it impractical to adjust the mineral Pb uptake results due to the various effects illustrated in Fig.4.

Figures 5 and 6 show the pH over time for the mineral-blank run in $NaNO_3$ and the mineral-Pb-blank in KNO_3. The shape of the pH curve for the mineral-blank in $NaNO_3$ is fairly typical of many of the actual runs with minerals, and it shows that H is evolved merely due to the presence of the filter paper reacting with the Pb. The effluent pH is lower than pH 5.5 the pH of the influent. The mineral-Pb-blank experiment does eventually return to an effluent of pH 5.5 at the end of the experiment. Unfortunately, the total H evolved in both of these blanks makes it impossible to calculate the amount of H evolved relative to the amount of Pb sorbed in the actual experimental runs or to calculate a mass balance for Pb, Mn, and H.

3.3 Mn Release

We did observe the release of Mn with or without the presence of Pb in the cryptomelane samples (data not shown). However, Mn was not released from birnessite in the presence of Pb. Unfortunately, problems with the ICP samples for the pyrolusite Mn analysis precluded us from determining if there was any Mn release for pyrolusite. It is likely that the cryptomelane samples were undergoing slow dissolution under our experimental conditions.

Other studies show Mn-release to various levels according to the specific mineral used and the experimental apparatus and conditions for that run. McKenzie (1980) saw less than 0.05% Mn released of the amount of metal ion adsorbed with several birnessite and cryptomelane samples that were reacted with Pb as well as other metals. Matocha et al. (2001) observed increased Mn release with increasing Pb adsorption from 0 at 0.1 mmol g^{-1} Pb adsorption to 0.09 mmol g^{-1} Mn released when 1.33 mmol g^{-1} Pb was adsorbed to birnessite. McKenzie (1979) also observed very little Mn released when Pb was reacted with hydrous manganese oxide at pH 4 for 24 h in a 0.02 M ionic strength solution. All of these studies were conducted at lower pH values using batch experiments; McKenzie (1980) worked at pH 5 with manual pH adjustments at an ionic strength of 0.001 M KNO_3 while Matocha et al. (2001) worked at pH 3.5 at an ionic strength of 0.01 M $NaClO_4$, and McKenzie (1979) at pH 4 in a 0.02 M ionic strength solution. As mentioned in the IEP discussion, dissolution of birnessite can occur below pH 3.5 (Murray, 1974) despite its stability.

3.4 pH

Figure 7 shows a fairly typical pH response for one of the full experimental runs with mineral rather than one of the types of blank runs. Figure 7 displays the Pb sorbed in terms of the cumulative volume passed through the reactor on the primary reactor whereas the secondary axis shows the pH of the effluent over time (arrows are directed from data to the appropriate axis). This particular run is synthetic cryptomelane in $NaNO_3$ background electrolyte. This solid is one of the more reactive solids and thus the initial equilibration of the pH is more dramatic. Most of the pH trends follow that shown in this plot with the pH usually dropping as most of the reaction takes place and then recovering back to the influent level after the Pb sorption levels off.

3.5 Lead Sorption on Manganese and Iron Oxides

Figure 8 shows the data for the total Pb sorption to the Mn-oxides in both $NaNO_3$ and KNO_3 background electrolytes, and Fig. 9 shows the data for the total Pb sorption to Fe-oxides in the same format. The data is normalized to the BET surface area of the mineral sample in that run. Figure 10 displays the mean of the replicates displayed in Figs. 8 and 9 along with the standard error of the mean. The statistics have limited value as they were generated from triplicates at best but often duplicates. In Fig. 10, the Fe-oxides are shown on the left, and the Mn-oxides are shown on the right. White bars denote $NaNO_3$ runs, and gray bars denote KNO_3 experiments.

Figure 10 clearly shows that some Mn-oxides, once normalized to surface area, sorb significantly more Pb than Fe-oxides. Synthetic birnessite removes almost an order of magnitude more Pb from solution than the Fe-oxides do. However, the natural pyrolusite Py8 and the natural cryptomelanes, Cr1 and especially Cr 2, remove a similar amount of Pb from solution as many of the natural and synthetic Fe-oxides.

All the Fe-oxides run in this study sorb fairly similar amounts of Pb once normalized to surface area. Also, there are not any clear trends between the synthetic and natural Fe-oxides. However, it is interesting to note that synthetic akaganeite, especially in the $NaNO_3$ matrix, has a particularly low affinity for Pb.

The synthetic Mn-oxides do have higher affinities for Pb than the natural Mn-oxides. The synthetic and natural pyrolusites have particularly striking differences whereas the cryptomelanes are not nearly so drastic. The general order of sorption in KNO_3 is Nat. cryptomelane, Cr2 ≈ Nat. pyrolusite, Py8 < Nat. cryptomelane, Cr1 < Syn. cryptomelane ≈ Syn. pyrolusite < Syn. birnessite. The order is slightly different in the $NaNO_3$ background electrolyte with Nat. pyrolusite, Py8 < Nat. cryptomelane, Cr2 ≈ Nat. cryptomelane, Cr1 < Syn. cryptomelane ≈ Syn. pyrolusite << Syn. birnessite.

Synthetic akaganeite, goethite, and ferrihydrite show differences beyond experimental error in Pb sorption in different electrolyte solutions. These three synthetic Fe-oxide solids all had lower affinities for Pb in the $NaNO_3$ bathing solution. Of the Mn-oxides Nat. pyrolusite Py8, Nat. cryptomelane Cr1, and Syn. birnessite displayed differences beyond experimental error in Pb sorption among their different electrolytes. Natural pyrolusite and Nat. cryptomelane Cr2 results indicated increased Pb sorption in a KNO_3 solution environment whereas the Syn. birnessite reacted more strongly with Pb in the presence of the $NaNO_3$ electrolyte.

Comparing the sorption trends in Fig. 9 to the IEP data shown in Table 2, we see that a few of the points do show agreement between the IEP magnitude and the amount of sorption; for example, the very low IEP of the synthetic birnessite agrees with its very high affinity for Pb. However, the overall IEP trends do not match up with the sorption affinity series given above (noting that a lower IEP would mean a more negative surface and therefore more attraction for the Pb^{2+} ion). Additionally, the Nat. pyrolusite Py8 and the Nat. cryptomelane Cr1 electrolyte sorption trends in the two electrolytes do not coordinate with the IEP values. Both the Py8 and Cr1 show increased sorption in the KNO_3 electrolyte despite the solid having higher IEP values in the potassium electrolyte. However, many studies note that the operative mechanism of Pb removal from solution by Mn-oxides is specific adsorption (Manceau et al., 1997; Manceau et al., 2002; Matocha et al., 2001; Morin et al., 1999; Ostergren et al., 1999).

3.6 FE-SEM

Low voltage, nanometer resolution FE-SEM images are shown in Figs. 11 and 12 of the synthetic birnessite and synthetic cryptomelane samples as examples. The morphology of the synthetic K-birnessite sample resembles that of a baerite rose. Yang and Wang (2002) showed a fairly similar SEM image of a randomly stacked synthetic birnessite. However, our XRD data clearly showed a peak at 7.20 Å, indicating that we do not have randomly stacked birnessite. Matocha et al. (2001) used the same synthesis method as used I this study to make K-birnessite and regarded their solid as being structurally similar to hexagonal birnessite. The synthetic cryptomelane sample exhibits hexagonal platelets. Only one image is shown for each of these solids because the before and after images were virtually identical as we did not observe any microprecipitates on the reacted solids. Additionally, there were no noticeable dissolution features on the solids. Manceau et al. (1992) claimed that Pb multinuclear surface complexes were forming on birnessite; however, Manceau et al. (2002) did not see any evidence of surface precipitation when they studied Pb and other metals reacting with various synthetic birnessite samples using polarized and extended X-ray absorption fine structure (EXAFS) spectroscopy. Matocha et al. (2001), using EXAFS, also did not discover surface precipitates on synthetic birnessite or manganite.

Figures 13 and 14 are FE-SEM images of unreacted natural cryptomelane Cr1 and natural cryptomelane Cr2 samples. Once normalized to surface area, one might expect that these solids would sorb more than the synthetic cryptomelane, which has flat hexagonal platelets, due to their increased microtopography. However, as seen by Fig. 10, the opposite is true. The

microtopography may not be playing a major role in determining the sorption efficiencies of the solids because different crystallographic faces are exposed in the natural, micronized samples versus the synthetic samples.

3.7 EDS

Figure 15 shows the EDS spectrum of the natural cryptomelane Cr1 before reaction with Pb. Figure 15 shows that Cr1 does have some Si, and Al present as well as Ba. It isn't surprising to see some Ba in the natural sample because in nature the hollandite group, of which cryptomelane is a member, generally are solid solutions rather than pure end members; hollandite itself has primarily Ba in its tunnels. Manganese, K, and O are present as expected. The EDS spectrum for Cr2 is very similar (data not shown) to the Cr1 spectrum. Once again Al and Si are present so it is possible that we may be seeing some additional phases or compositional impurities that were not displayed in the X-ray diffraction data. These impurities as mentioned earlier would effect the IEP of the solid and possibly the available reactive sites on the solid. These compositional impurities may account for the differences in the sorption of the natural versus the synthetic Mn-oxides.

3.8 XPS

Figure 16 shows the XPS survey scan of unreacted synthetic birnessite that was equilibrated in 0.01 M KNO_3 matrix solution before run in a Pb sorption experiment. Also shown are synthetic birnessite, natural cryptomelane Cr1, and synthetic cryptomelane after being run in a Pb sorption experiment using the $NaNO_3$ background electrolyte. As expected, the unreacted synthetic birnessite sample shows K but no Pb in the XPS spectrum. Remembering that we synthesized a potassium birnessite and that cryptomelane has K as the major tunnel cation, it is interesting that K is no longer present on the surface of the reacted birnessite and cryptomelane run in $NaNO_3$ electrolyte, but Na is. This clearly indicates that the K has exchanged with the Na, at least as far as surface analysis is concerned in these samples.

Table 3 compares the solution data results from the $NaNO_3$ flow study to the Pb surface enrichment information from the XPS high energy resolution scans (data not shown). The table displays the Pb/Mn atomic ratio along with the total Pb uptake after sorption runs for synthetic cryptomelane, natural cryptomelane Cr1, natural cryptomelane Cr2 and synthetic birnessite. Looking at the Pb/Mn ratios, synthetic cryptomelane has the most Pb enriched at the surface, followed by natural cryptomelane Cr1, and then finally the natural cryptomelane Cr2 and synthetic birnessite having the least amount of Pb enriched at the surface. Interestingly, synthetic birnessite removed the most Pb from solution (referring to our aqueous flow-studies). Because XPS is surface sensitive, it cannot "see" the interlayer of the birnessite structure. Therefore, we can conclude that most of the Pb is in the interlayer of the birnessite structure. This clearly suggests that the high sorption efficiency of the birnessite is probably due to the additional reactive sites in the interlayer of the solid. Similarly, the synthetic cryptomelane sorbed by far the most Pb relative to the two natural ones, yet the Pb/Mn surface ratio is only slightly higher for the synthetic sample. Therefore, Pb has probably entered the synthetic cryptomelane tunnels.

3.9 XRD

The reacted synthetic birnessite in both matrices and the synthetic cryptomelane in KNO_3 were X-rayed again (data not shown) after reaction to see if there were any observable phase changes. The samples were X-rayed on the filter paper with just the limited sample that was used in the reactor. A filter paper alone was also X-rayed. The filter paper alone did cause a noticeable background hump; this hump made it particularly difficult to examine the birnessite

spectrum. However, the 7.20 Å peak is reduced to 7.06 Å for the reacted sample in the $NaNO_3$ matrix and 6.89 Å for the reacted sample in the KNO_3 matrix. The reacted cryptomelane phase still X-rayed as cryptomelane but some of the peaks seemed slightly sharper. Potassium-birnessite has a basal spacing of 7.2 Å (Golden et al., 1986; Feng et al., 1998), and Golden et al. (1986) noted a 7.16 Å basal spacing for hydrated Na-birnessite (only 7.07 Å if in vacuum); However, Golden et al. (1986) noted a basal spacing for K-birnessite of only 7.13 Å.

Other studies using X-ray diffraction data have also shown evidence of Pb uptake into the interlayer of birnessite (Van der Weijden and Kruissink, 1977; McKenzie, 1980). McKenzie (1980) saw that the reaction of Pb with different birnessite samples either reduced the basal spacings as shown in our X-ray diffraction data or completely destroyed the spacings. EXAFS studies revealed that Pb(II) formed inner-sphere, corner-sharing complexes located above and below vacancies in the MnO_2 layers (Morin et al., 1999; Matocha et al., 2001) and using polarized and extended XAFS Manceau et al. (2002) specifically noted octahedral tridentate corner-sharing complexes with Pb and the birnessite interlayer. Manceau et al. (2002) also noted that the EXAFS data is consistent with the formation of octahedral, tridentate edge-sharing interlayer complexes.

3.10 Reactions in Interlayers and Tunnel Structures

Several authors have noted that birnessite readily participates in cation exchange reactions (see Ching and Suib, 1997; Post, 1992; Brock et al., 1998). However, experiments have shown that the extent of exchange is dependent upon the nature of the cation and the hydration, or lack thereof, of the interlayer (Golden et al., 1986; Ching and Suib, 1997; Brock et al., 1998). In fact, Golden et al. (1986) noted that when K, Sr, and La birnessites were heated at 105 °C under vacuum for 12 h, the solids would no longer participate in exchange reactions; Li, Na, Ca, and Ni birnessite still participated in exchange reactions after the same treatment. The authors therefore attributed low cation exchange capacity of natural birnessites to the presence of fixed cations.

Members of the hollandite group such as cryptomelane are referred to by some authors as molecular sieves and it is often noted that the cryptomelane tunnel structures are capable of fixing metal ions with an effective ionic radius of approximately 1.4 Å into 4.6 Å tunnels (Feng et al., 1995a; Feng et al., 1995b; Ching and Suib, 1997; Brock et al., 1998). The ionic radii for K^+ is 1.33 Å, Pb^{2+} 1.20 Å, Mn^{2+} 0.80 Å, Na^+ 0.95 Å, Mn^{4+} 0.50 Å, and water is 1.38 Å (Bystrom and Bystrom, 1950; Murray, 1975; Van der Weijden and Kruissink, 1977). It makes sense that K is particularly suited towards the solid and that in hollandite and cryptomelane K occupies a "special position", a cavity formed by 8 O atoms at the corners of a distorted prism, whereas Pb(II) would be displaced (Post et al., 1982). Bystrom and Bystrom (1950) followed by Van der Weijden and Kruissink (1977) discuss that larger ions such as K keep the cryptomelane structure from collapsing; however the K ion is somewhat too large for the structure because of the short distance between equivalent sites that accommodate the ions. Thus these authors concluded that this rationale could explain the higher exchange capacity of smaller ions, and would mean that Pb would be favored over K in an exchange reaction. Van der Weijden and Kruissink (1977) found that Pb was preferentially sorbed to birnessite, but it was not favored by poorly crystalline cryptomelane, which favored larger Ba instead. Perseil and Giovanoli (1988) studied the hollandite group including intermediate members and suggested that substitution may occur in favor of the higher valence ions. McKenzie (1980) did not see a coronodite pattern for the Pb-reacted cryptomelane XRD sample, which is what one would expect if Pb significantly replaced K in the tunnels of the cryptomelane structure. Feng et al. (1995a,b) notes that the K in

cryptomelane can be topotactically extracted, but it must be done in the presence of an acid. Obviously, a tunnel structure (especially a more compact tunnel structure Giovanoli and Brutsch, 1979) is much less likely to undergo exchange than a layer structure.

4 CONCLUSIONS

The leading conclusion from this systematic study, based on natural and synthetic species of seven Mn- and Fe-oxides in two background electrolytes, is that Mn-oxides are generally more efficient sorbents of Pb than Fe-oxides. With the exception of synthetic pyrolusite (see below), our results clearly suggest that this efficiency is directly related to internal reactive sites in the structures of Mn-oxides that contain them (birnessite and cryptomelane, in our case). Layer structures such as birnessite have the highest Pb sorption efficiency, while a 2 x 2 tunnel structure such as cryptomelane has lower efficiencies than birnessite, but higher efficiencies than other Mn- or Fe-oxide structures without internal reactive sites. The tunnel structures are likely more limited in efficiency than layer structures due to the steric restrictions of tunnels, which are not even cross-linked as exhibited, for example, by many zeolites.

Other final results include the fact that synthetic birnessite, pyrolusite, and cryptomelane have higher sorption efficiencies for Pb than natural Mn-oxides or natural and synthetic Fe-oxide minerals tested in this study. Two natural cryptomelanes can also sorb Pb more efficiently than the natural or synthetic Fe-oxides tested. Overall, only the natural pyrolusite tested clearly had a sorption efficiency as low as the Fe-oxides, but one of the two natural cryptomelane samples did approach similar values. Most of the natural and synthetic Fe-oxides examined in this study removed about the same amount of Pb from solution once normalized to surface area, although synthetic akaganeite and hematite were significantly less reactive than the rest.

There are a number of reasons why synthetic samples might be more or less reactive than natural ones (e.g. differences in impurities, surface composition, crystal form, microtopography, and crystal size). In the case of cryptomelane, this difference may be due to tunnel exchange kinetics. The synthetic cryptomelane, which sorbed up to twice the Pb as the natural cryptomelanes in these experiments, has only K in its 2 x 2 tunnels at the beginning of the experiments. The natural samples have both K and Ba. Barium-oxygen bonds in the tunnels have considerably higher bond strengths relative to K-O bonds, and the exchange and passage of Pb in the tunnels would be expected to be faster in the latter case where each Pb exchanges for two K's. The fact that the synthetic pyrolusite sorbs considerably more Pb than the natural variety tested, and that its Pb sorption efficiency is so high overall, remains a mystery. Pyrolusite has a framework structure, without internal reaction sites like cryptomelane. The only unusual feature of this sample was its very low surface area, by far the lowest of all samples used in this study. Otherwise, its XRD pattern and composition were nominal.

Lead was shown to go into the interlayer of synthetic birnessite by comparing solution sorption data to XPS surface enrichment calculations; similar approaches suggest that Pb may be able to go into the tunnels of some cryptomelane samples, but the data is not conclusive. X-ray diffraction data did show that the interlayer spacing of the birnessite was decreasing as expected for Pb substitution. X-ray diffraction did not show a coronadite pattern replacing the cryptomelane pattern with Pb sorption; this is most likely because not enough Pb replaced the K in the interlayer to form coronadite in such a short experiment (approx. 5 hours) at low temperature. Supporting this, coronadite as well as hollandite are generally formed under hydrothermal processes whereas cryptomelane is generally formed near oxidation zones (Perseil

and Giovanoli, 1988). Coronadite and hollandite seem to only be formed when the Pb and Ba ions get into the tunnel structure and are "fixed" with the aid of higher temperatures.

The sorption data did not fully agree with the IEP data suggesting specific chemical interactions dominate over electrostatic reactions in Pb sorption to the solids studied. This agrees with the current findings in the literature that Pb specifically sorbs as inner sphere complexes to Fe and Mn-oxides. Additionally, background electrolytes cannot be considered inert in the presence of Mn-oxides as seen by the increase in the IEP data when going from $NaNO_3$ to KNO_3 electrolytes and the exchange of K for Na determined from the XPS data. The increased sorption of birnessite in the $NaNO_3$ matrix compared to the KNO_3 matrix is most likely due to Na being smaller and more labile and thus allowing Pb to exchange into the interlayer of the birnessite more easily.

This study strongly suggests that mobilized Pb in soils can be efficiently retained by Mn-oxides with internal reactive sites occupied by alkali cations, which can readily exchange out for Pb. Such strategies could be utilized in the future where Pb-contaminated sites are undergoing remediation.

5 REFERENCES

Aualiitia T. U. and Pickering W. F. (1987) The Specific Sorption of Trace Amounts of Cu, Pb, and Cd By Inorganic Particulates. *Water Air and Soil Pollution* **35**(1-2), 171-185.

Balistrieri L. S. and Murray J. W. (1982) The surface chemistry of δ-MnO_2 in major ion seawater. *Geochimica et Cosmochimica Acta* **46**, 1041-1052.

Balistrieri L. S. and Murray J. W. (1986) The surface chemistry of sediments form the Panama Basin: the influence of Mn oxides on metal adsorption. *Geochimica et Cosmochimica Acta* **50**, 2235-2243.

Boeckx R. L. (1986) Lead Poisoning in Children. *Analytical Chemistry* **58**(2), 274A-287A.

Brock S. L., Duan N. G., Tian Z. R., Giraldo O., Zhou H., and Suib S. L. (1998) A review of porous manganese oxide materials. *Chemistry of Materials* **10**(10), 2619-2628.

Buck Scientific I. (1992) Model 200A atomic absorption spectrophotometer flame system-instruction manual. Buck Scientific, Inc.

Buhrke V. E., Jenkins R., and Smith D. K. (1998) A practical guide for the preparation of specimens for X-ray fluorescence and X-ray diffraction analysis. John Wiley & Sons, Inc.

Burns R. G. (1976) The uptake of cobalt into ferromanganese nodules, soils, and synthetic manganese (IV) oxides. *Geochemica et Cosmochimica Acta* **40**, 95-102.

Burns R. G. and Burns V. M. (1979) Manganese oxides. In *Marine Minerals*, Vol. 6 (ed. R. G. Burns), pp. 1-40. Mineralogical Society of America.

Bystrom A. and Bystrom A. M. (1950) The crystal structure of hollandite, the related manganese oxide minerals, and α-MnO_2. *Acta Crystallographica* **3**, 146-154.

Carpenter R. H., Pope T. A., and Smith R. L. (1975) Fe-Mn oxide coatings in stream sediment geochemical surveys. *Journal of Geochemical Exploration* **4**, 349-363.

Chao T. T. and Theobald P. K. (1976) The significance of secondary ion and manganese oxides in geochemical exploration. *Economic Geology* **71**, 1560-1569.

Ching S. and Suib S. L. (1997) Synthetic routes to microporous manganese oxides. *Comments On Inorganic Chemistry* **19**(5), 263-282.

Chlopecka A. and Adriano D. C. (1997) Influence of zeolite, apatite and Fe-oxide on Cd and Pb uptake by crops. *the Science of the Total Environment* **207**, 195-206.

Cornell R. M. and Schwertmann U. (1996) *The iron oxides: structures, properties, reactions, occurrence and uses*. VCH Publishers.

Dahal M. P. and Lawrance G. A. (1996) Adsorption of thallium(I), lead(II), copper(II), bismuth(III) and chromium(III) by electrolytic manganese dioxide. *Adsorption Science & Technology* **13**(4), 231-240.

Davies B. E. (1995) Lead. In *Heavy Metals in Soils* (ed. B. J. Alloway), pp. 206-223. Chapman & Hall.

Dixon J. B. and Skinner H. C. W. (1992) Manganese minerals in surface environments. In *Biomineralization processes of iron and manganese: modern and ancient environments*, Vol. 21 (ed. H. C. W. Skinner and R. W. Fitzpatrick), pp. 51-73. Catena Verlag.

Dong D., Li Y., Zhang B., Hua X., and Yue B. (2001) Selective chemical extraction and separation of Mn, Fe oxides and organic material in natural surface coatings: application to the study of trace metal adsorption mechanism in aquatic environments. *Mirochemical Journal* **69**, 89-94.

Dong D. M., Nelson Y. M., Lion L. W., Shuler M. L., and Ghiorse W. C. (2000) Adsorption of Pb and Cd onto metal oxides and organic material in natural surface coatings as determined by selective extractions: new evidence for the importance of Mn and Fe oxides. *Water Research* **34**(2), 427-436.

Feng Q., Kanoh H., Miyai Y., and Ooi K. (1995a) Alkali-Metal Ions Insertion/Extraction Reactions With Hollandite-Type Manganese Oxide in the Aqueous-Phase. *Chemistry of Materials* **7**(1), 148-153.

Feng Q., Kanoh H., Miyai Y., and Ooi K. (1995b) Hydrothermal Synthesis of Lithium and Sodium Manganese Oxides and Their Metal-Ion Extraction Insertion Reactions. *Chemistry of Materials* **7**(6), 1226-1232.

Feng Q., Yanagisawa K., and Yamasaki N. (1998) Hydrothermal soft chemical process for synthesis of manganese oxides with tunnel structures. *Journal of Porous Materials* **5**(2), 153-161.

Frondel C., Marvin U. B., and Ito J. (1960) New data on birnessite and hollandite. *The American Mineralogist* **45**, 871-875.

Gadde R. R. and Laitinen H. A. (1974) Studies of heavy metal adsorption by hydrous iron and manganese oxides. *Analytical Chemistry* **46**(13), 2022-2026.

Gilmore E. A., G.J. Evans, and M.D. Ho. (2001) Radiochemical assessment of the readsorption and redistribution of lead in the SM&T sequential extraction procedure. *Analytica Chimica Acta* **439**, 139-151.

Giovanoli R. (1980) Vernadite is random-stacked birnessite. *Mineral. Deposita* **15**, 251-253.

Giovanoli R. and Brutsch R. (1979) L'echange des ions de transition par le manganate- 10 A et le manganate 7 A. In *La Genese Des Nodules De Manganese*, Vol. 289 (ed. C. I. d. C.N.R.S.), pp. 305-315. Colloques Internatonaux du C.N.R.S.

Golden D. C., Dixon J. B., and Chen C. C. (1986) Ion exchange thermal transformations and oxidizing properties of birnessite. *Clays and Clay Minerals* **34**(5), 511-520.

Goldstein J. I., Romig A. D., Jr., Newbury D. E., Lyman C. E., Echlin P., Fiori C., Joy D. C., and Lifshin E. (1992) *Scanning Electron Microscopy and x-ray microanalysis: a text for biologists, materials scientists, and geologists*. Plenum Press.

Gregson S. K. a. B. J. A. (1984) *Journal of Soil Science* **35**, 55-61.

Healy T. W., Herring A. P., and Fuerstenau D. W. (1966) The effect of crystal structure on the surface properties of a series of manganese dioxides. *Journal of Colloid and Interface Science* **21**, 435-444.

Hewett D. F. and Fleischer M. (1960) Deposits of the manganese oxides. *Economic Geology* **55**(1), 1-55.

Hudson-Edwards K. A. (2000) Heavy metal-bearing Mn oxides in river channel and floodplain sediments. In *Environmental Mineralogy: Microbial Interactions, Anthropogenic Influences, Contaminated Land and Waste Management*, Vol. 9 (ed. J. D. Cotter-Howells, L.S. Campbell, E. Valsami-Jones, M. Batchelder), pp. 207-226. Mineralogical Society of Great Britian & Ireland.

Jardine P. M., Zelazny L. W., and Evans A., Jr. (1986) Solution aluminum anomalies resulting from various filtering materials. *Soil Science Society of America Journal* **50**(4), 891-894.

Jenne E. A. (1968) Controls on Mn, Fe, Co, Ni, Cu, and Zn concentrations in soils and water: the significant role of hydrous Mn and Fe oxides. In *Trace inorganics in water*, Vol. 73 (ed. R. A. Baker), pp. 337-387. American Chemical Society.

Kabata-Pendias A. (1980) Heavy metals sorption by clay minerals and oxides or iron and manganese. *Mineralogia Polonica* **11**(2), 3-13.
Kaim W. (1994) *Bioinorganic chemistry: inorganic elements in the chemistry of life: an introduction and guide*. John Wiley & Sons.
Kosmulski M. (2001) *Chemical properties of material surfaces*. Marcel Dekker, Inc.
Langmuir D. (1997) *Aqueous environmental geochemistry*. Prentice-Hall, Inc.
Li Y. H. (1982) interelement relationship in abyssal Pacific ferromanganese nodules and associated pelagic sediments. *Geochimica et Cosmochimica Acta* **46**, 1053-1060.
Manceau A., Charlet L., Boisset M. C., Didier B., and Spadini L. (1992) Sorption and speciation of heavy metals on hydrous Fe and Mn oxides. From microscopic to macroscopic. *Applied Clay Science* **7**, 201-223.
Manceau A., Drits V. A., Silvester E., Bartoli C., and Lanson B. (1997) Structural mechanism of Co2+ oxidation by the phyllomanganate buserite. *American Mineralogist* **82**(11-12), 1150-1175.
Manceau A., Lanson B., and Drits V. A. (2002) Structure of heavy metal sorbed birnessite. Part III: Results from powder and polarized extended X-ray absorption fine structure spectroscopy. *Geochimica et Cosmochimica Acta* **66**(15), 2639-2663.
Matocha C. J., Elzinga E. J., and Sparks D. L. (2001) Reactivity of Pb(II) at the Mn(III,IV) (Hydr)Oxide-Water Interface. *Environmental Science and Technology* **35**, 2967-2972.
McBride M. B. (1994) *Environmental chemistry of soils*. Oxford University Press.
McCarty D. K., Moore J. N., and Marcus W. A. (1998) Mineralogy and trace element association in an acid mine drainage iron oxide precipitate; comparison of selective extractions. *Applied Geochemistry* **13**(2), 165-176.
McKenzie R. M. (1971) The synthesis of birnessite, cryptomelane, and some other oxides and hydroxides of manganese. *Mineralogical Magazine* **38**(296), 493-502.
McKenzie R. M. (1978) The effect of two manganese dioxides on the uptake of lead, cobalt, nickel, copper and zinc by subterranean c lover. *Aust J Soil Res* **16**(2), 209-214.
McKenzie R. M. (1979) Proton release during adsorption of heavy metal ions by a hydrous manganese dioxide. *Geochimica et Cosmochimica Acta* **43**(11), 1855-1858.
McKenzie R. M. (1980) The adsorption of lead and other heavy metals on oxides of manganese and iron. *Aust J Soil Res* **18**(1), 61-73.
McKenzie R. M. (1981) The surface charge on manganese dioxides. *Australian Journal of Soil Research* **19**, 41-50.
McKenzie R. M. (1989) Manganese Oxides and Hydroxides. In *Minerals in soil environments*, Vol. 1 (ed. J. B. Dixon and S. B. Weed), pp. 437-465. Soil Science Society of America.
Morin G., Ostergren J. D., Juillot F., Ildefonse P., Calas G., and Brown G. E. (1999) XAFS determination of the chemical form of lead in smelter- contaminated soils and mine tailings: Importance of adsorption processes. *American Mineralogist* **84**(3), 420-434.
Murray J. W. (1974) The surface chemistry of hydrous manganese dioxide. *Journal of Colloid and Interface Science* **46**(3), 357-371.
Murray J. W. (1975) The interaction of metal ions at the manganese dioxide-solution interface. *Geochimica et Cosmochimica Acta* **30**, 505-519.
Norrish K. (1975) Geochemistry and mineralogy of trace elements. In *Trace elements in soil-plant-animal systems* (ed. D. J. D. Nicholas and A. R. Egan), pp. 55-81. Academic Press.

Nriagu J. O. (1978) Lead in soils, sediments and major rock types. In *The biogeochemistry of lead in the environment: Ecological Cycles*, Vol. 1 A (ed. J. O. Nriagu), pp. 16-72. Elsevier/North-Holland Biomedical Press.

Ostergren J. D., Brown G. E., Parks G. A., and Tingle T. N. (1999) Quantitative speciation of lead in selected mine tailings from Leadville, CO. *Environmental Science & Technology* **33**(10), 1627-1636.

Parida K., Satapathy P. K., and Das N. (1996) Studies on Indian Ocean manganese nodules .4. Adsorption of some bivalent heavy metal ions onto ferromanganese nodules. *Journal of Colloid and Interface Science* **181**(2), 456-462.

Paulson A. J., Feely R. A., Curl H. C., Crecelius E. A., and Geiselman T. (1988) The Impact of Scavenging On Trace-Metal Budgets in Puget Sound. *Geochimica et Cosmochimica Acta* **52**(7), 1765-1779.

Perseil E. and Giovanoli R. (1988) Sur la variation de la composition ponctuelle des termes de las serie isostructurale: Cryptomelane-Hollandite-Cornodite et les conditions de gisement. *Schweiz. Mineral. Petrogr. Mitt.* **68**, 113-123.

Post J. E. (1992) Crystal structures of manganese oxide minerals. In *Biomineralization processes of iron and manganese: modern and ancient environments*, Vol. 21 (ed. H. C. W. Skinner and R. W. Fitzpatrick), pp. 51-73. Catena Verlag.

Post J. E., Von Dreele R. B., and Buseck P. R. (1982) Symmetry and cation displacements in hollandites: structure refinements of hollandite, cryptomelane and priderite. *Acta Crystallographica* **B38**, 1056-1065.

Rauch S., Morrison G. M., Motelica-Heino M., Donard O. F. X., and Muris M. (2000) Elemental association and fingerprinting of traffic related metals in road sediments. *Environmental Science & Technology* **34**(15), 3119-3123.

Rickard D. T. and Nriagu J. O. (1978) Aqueous environmental chemistry of lead. In *The biogeochemistry of lead in the environment: Ecological Cycles*, Vol. 1 A (ed. J. O. Nriagu), pp. 219-284. Elsevier/North-Holland Biomedical Press.

Rimstidt J. D. and Newcomb W. D. (1993) Measurement and analysis of rare data: The rate of reaction of ferric ion with pyrite. *Geochimica et Cosmochimica Acta* **57**, 1919-1934.

Schwertmann U. and Cornell R. M. (1991) *Iron oxides in the laboratory*. VCH Publishers.

Schwertmann U. and Taylor R. M. (1989) Iron oxides. In *Minerals in soil environments*, Vol. 1 (ed. J. B. Dixon and S. B. Weed), pp. 379-438. Soil Science Society of America.

Sparks D. L. (1995) *Environmental soil chemistry*. Academic Press.

Tampouris S., N. Papassiopi, I. Paspaliaris. (2001) Removal of contaminated metals from fine grained soils, using agglomeration, chloride solutions and pile leaching techniques. *Journal of Hazardous Materials* **B84**, 297-319.

Taylor R. M., McKenzie R. M., and Norrish K. (1964) The mineralogy and chemistry of manganese in some Australian soils. *Australian Journal of Soil Research* **2**, 235-248.

Taylor R. M. and R.M. M. (1966) The association of trace elements with manganese minerals in Australian soils. *Aust. J. Soil Res.* **4**, 29-39.

Van der Weijden C. H. and Kruissink E. C. (1977) Some geochemical controls on lead and barium concentrations in ferromanganese deposits. *Marine Chemistry* **5**, 93-112.

Waltham C. A. and Eick M. J. (2002) Kinetics of arsenic adsorption on goethite in the presences of sorbed silicic acid. *Soil Science Society of America Journal* **66**, 818-825.

Weaver R. (2001) Comparison of the reactivity of various Mn-oxides with Cr(III) aqueous: microscopic and spectroscopic observations of dissolution, Cr-sorption and Cr & Mn

redox interactions. electronic dissertation, Virginia Polytechnic Institute and State University.
webmineral.com. (2002) Akaganeite Mineral Data, Vol. 2002.
Welz B. and Sperling M. (1999) *Atomic absorption spectrometry*. Wiley-VCH.
Yang D. S. and Wang M. K. (2002) Synthesis and characterization of birnessite by oxidizing pyrochroite in alkaline conditions. *Clays and Clay Minerals* **50**(1), 63-69.
Yousef A. A., Arafa M. A., and Malati M. A. (1971) Adsorption of sulphite, oleate and manganese (II) ions by β-manganese dioxide and its activation in flotation. *Journal of Applied Chemical Biotechnology* **21**, 200-207.
Zelazny L., He L., and Vanwormhoudt A. (1996) Charge Analysis of Soils and Anion Exchange. In *Methods of Soil Analysis: Chemical Methods*
Part 3, Vol. 5 (ed. D. L. Sparks), pp. 1231-1253. Soil Science Society of America.

6 TABLES

Table 1. Summary of chemical and structural properties of the Mn and Fe-oxides used in this study.

Mineral	Abbreviation Used in Text and Figures	General Formula	Lending Institution Or Synthesis Reference	Origin or Synthesis Method	Structure	BET, N_2 Surface Area m^2/g	Matching JCPDS File(s)
Mn-oxides							
Natural							
Cryptomelane	Cr1	$K_{1.3-1.5}(Mn^{4+}Mn^{3+})_8O_{16}$[a]	NMNH	Sitpar Mn Mine, Chindara, India	2X2 tunnel	5.3	44-1386,
	Cr2		VPI	unknown		14.9	44-1386, 42-1348
Pyrolusite	PY8	MnO_2[a]	VPI	unknown	1X1 tunnel	7.9	[Weaver, 2001]
Synthetic							
Birnessite		$K_4Mn_{14}O_{27}•9H_2O$[b]	[McKenzie, 1971]	heated reduction of $KMnO_4$ with HCl	layer	35.4	23-1239
Cryptomelane, α-MnO_2		$K_{1.3-1.5}(Mn^{4+}Mn^{3+})_8O_{16}$[a]	[McKenzie, 1971]	Convert birnessite by ignition	2X2 tunnel	25.7	42-1348, 44-1386
Pyrolusite, β-MnO_2		MnO_2[a]	[McKenzie, 1971]	Ignition of evaporated manganous nitrate	1X1 tunnel	0.15	81-2261,72-1984, 24-0735
Fe-oxides							
Natural							
Hematite	M2258	α-Fe_2O_3	VPI	Clinton, NY		8.2	87-1165
	D61		VPI	Rio Marina Mine, Rio Marina, Isula D'Elba, Italy		4.6	87-1165
Goethite	Fe11	α-FeOOH	Private donor	Pikes peak batholith		4.0	29-0713

Synthetic					
Hematite, α-Fe_2O_3	α-Fe_2O_3	[Schwertmann, 1991]	Method 1, forced hydrolysis of Fe(III) salt	42.5	87-1165
Goethite, α-FeOOH	α-FeOOH	[Schwertmann, 1991]	Fe(III) alkaline system, heated	76.3	[Waltham, 2002]
Ferrihydrite (6-line)	$Fe_5OH_{8.}\cdot 4H_2O$[c]	[Schwertmann, 1991]	Hydrolysis of acidic Fe(III) solution	193.3	29-0712
Akaganeite, β-FeOOH	$FeO_{0.8}(OH)_{1.2}Cl_{0.2}$[d]	[Schwertmann, 1991]	Hydrolysis of acidic $FeCl_3$	116.4	34-1266,42-1315

a) [Post, 1992]
b) [Burns, 1976] assuming equal substitution of K for Na given in original formula.
c) [Schwertmann, 1991]
d) [webmineral.com, 2002]

Table 2. Estimated Isoelectric Points, IEP, of the Mn and Fe-oxy(hydr)oxides used in this study.

Solids	0.01 M Matrix $NaNO_3$	0.01 M Matrix KNO_3
Fe-oxy(hydr)oxides		
Nat. Hematite, M2258	<4.0	<4.0
Nat. Hematite, D61	6.8	6.8
Nat. Goethite, Fe11	7.0	6.7
Syn. Akaganeite	6.6	≥6.7
Syn. Hematite	7.3	7.2
Syn. Goethite[a]	9.2	Not measured
Syn. Ferrihydrite	6.8	6.9
Mn-oxides		
Nat. Pyrolusite, Py8	4.9	6.5
Nat. Cryptomelane, Cr2	6.2	≥6.8
Nat. Cryptomelane, Cr1	4.3	6.7
Syn. Cryptomelane	≤6.0	6.2
Syn. Pyrolusite	≤4.3	6.5
Syn. Birnessite	<2.0	<2.0

a) Personal communication Luxton, T. and Eick, M. 2002

Table 3. Comparison of Pb sorption data from flow study to XPS data in the $NaNO_3$ background electrolyte.

	Nat. Cryptomelane, Cr1	Nat. Cryptomelane, Cr2	Syn. Cryptomelane	Syn. Birnessite
Total Pb after 5 h ($umol/m^2$)	1.46	2.72	6.95	12.38
Pb/Mn Atomic Ratio (XPS)	0.08	0.06	0.09	0.06

7 FIGURES

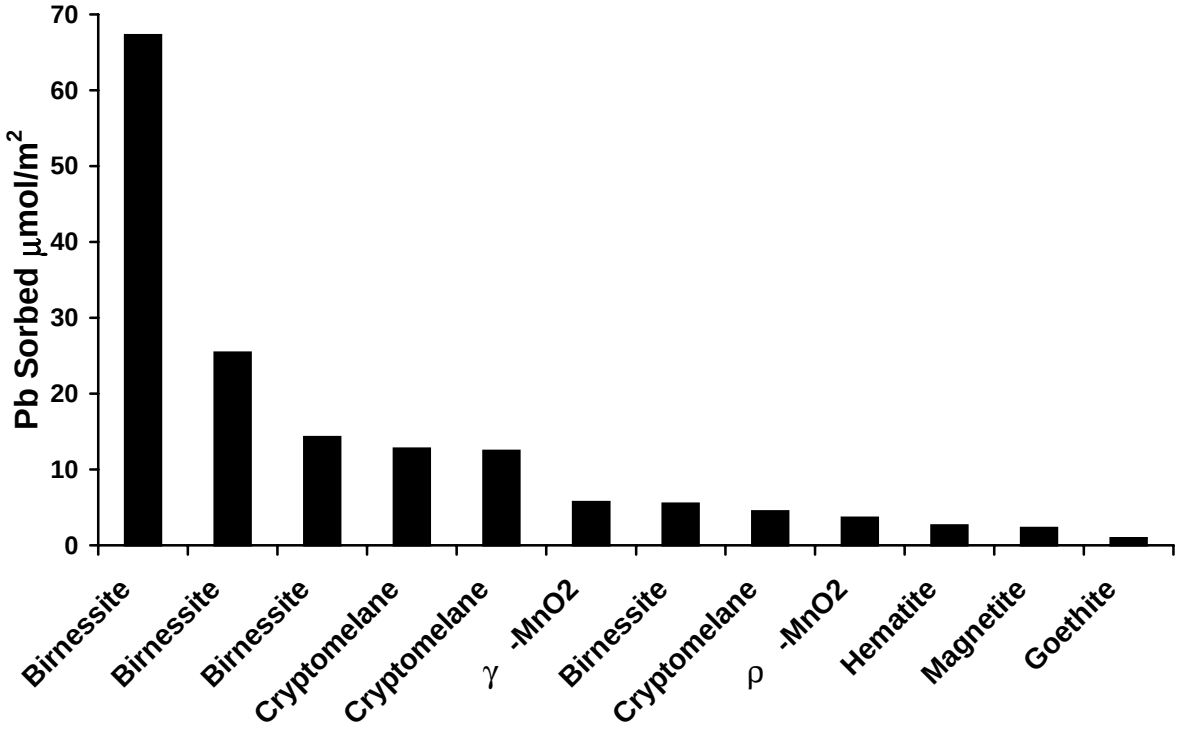

Fig. 1. Lead sorption to Mn and Fe-oxides in terms of surface area of the solid. Adapted from McKenzie (1980). The same phase is listed more than once because these solids were prepared using different synthesis methods.

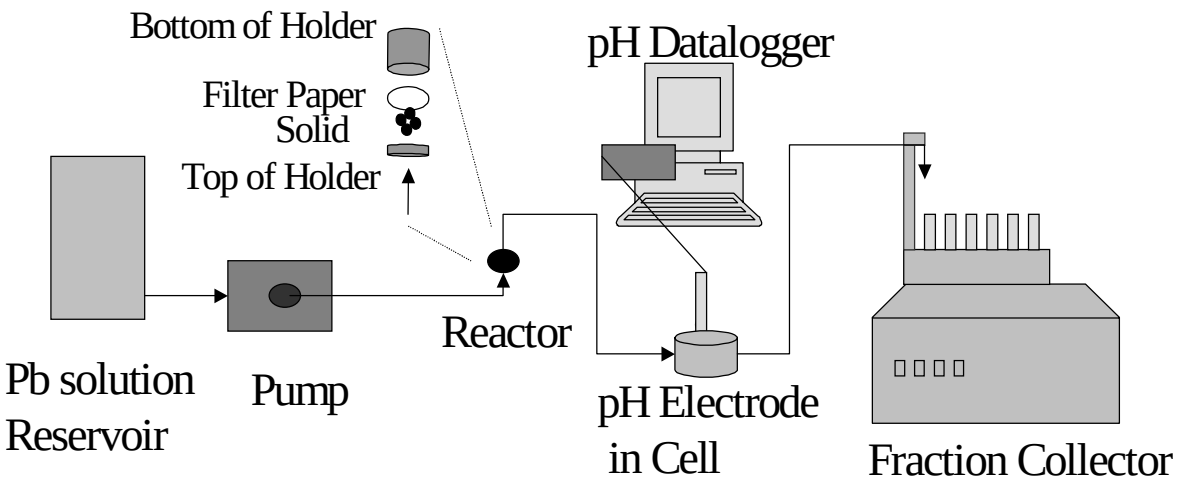

Fig. 2. Schematic of sorption flow study showing the components of the experiment and the direction of flow.

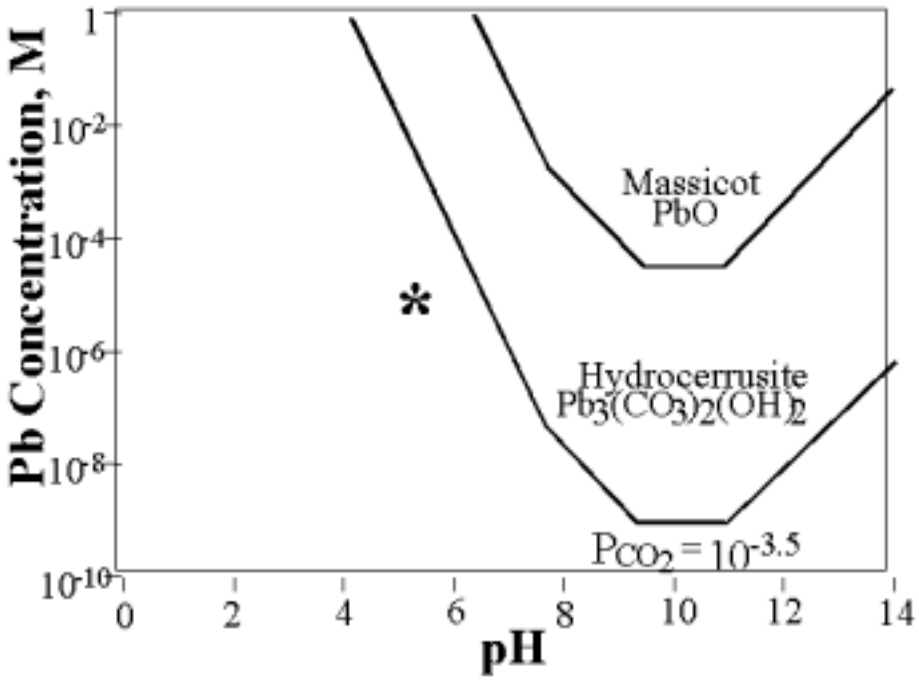

Fig. 3. Lead solubility diagram showing pH and Pb concentration at which the lead solids massicot and hydrocerrusite form at atmospheric carbonate levels. The asterisk approximately indicates the pH and Pb concentration conditions of this study. The thermodynamic data was obtained from Garrels and Christ, 1965 [Garrels, 1965].

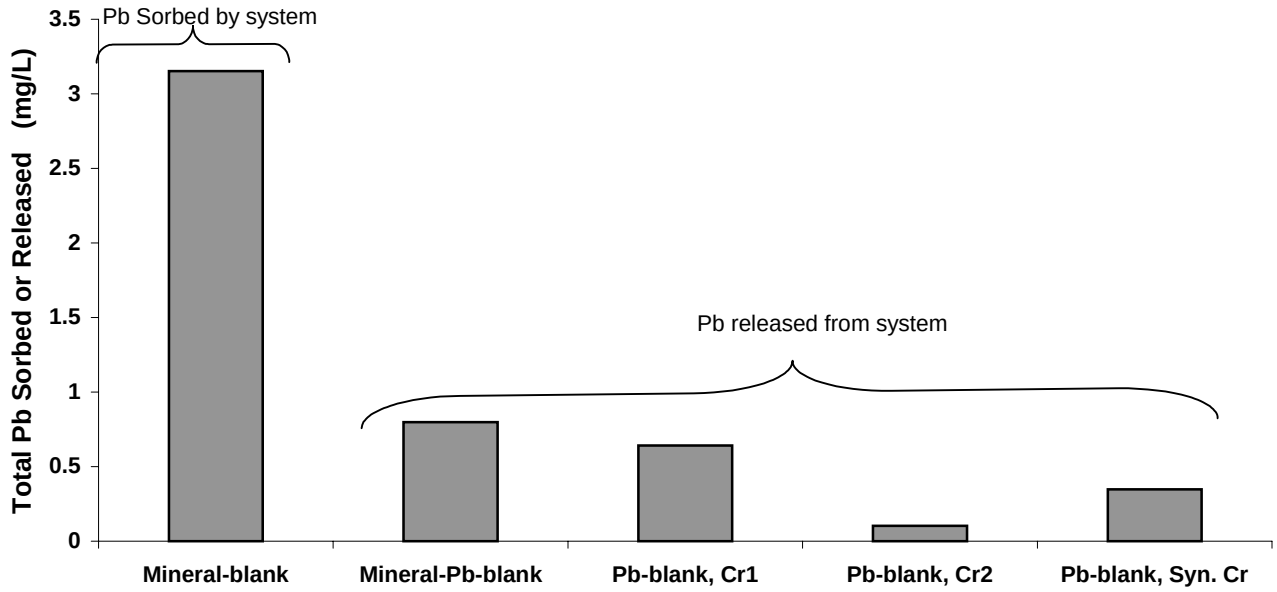

Fig. 4. "Blank" flow system experiments in KNO_3 background electrolyte. The chosen filter paper is present in all experiments by design. The data is NOT normalized to surface area because the first two "blank" experiments do not have a mineral sample in the system see text for further details.

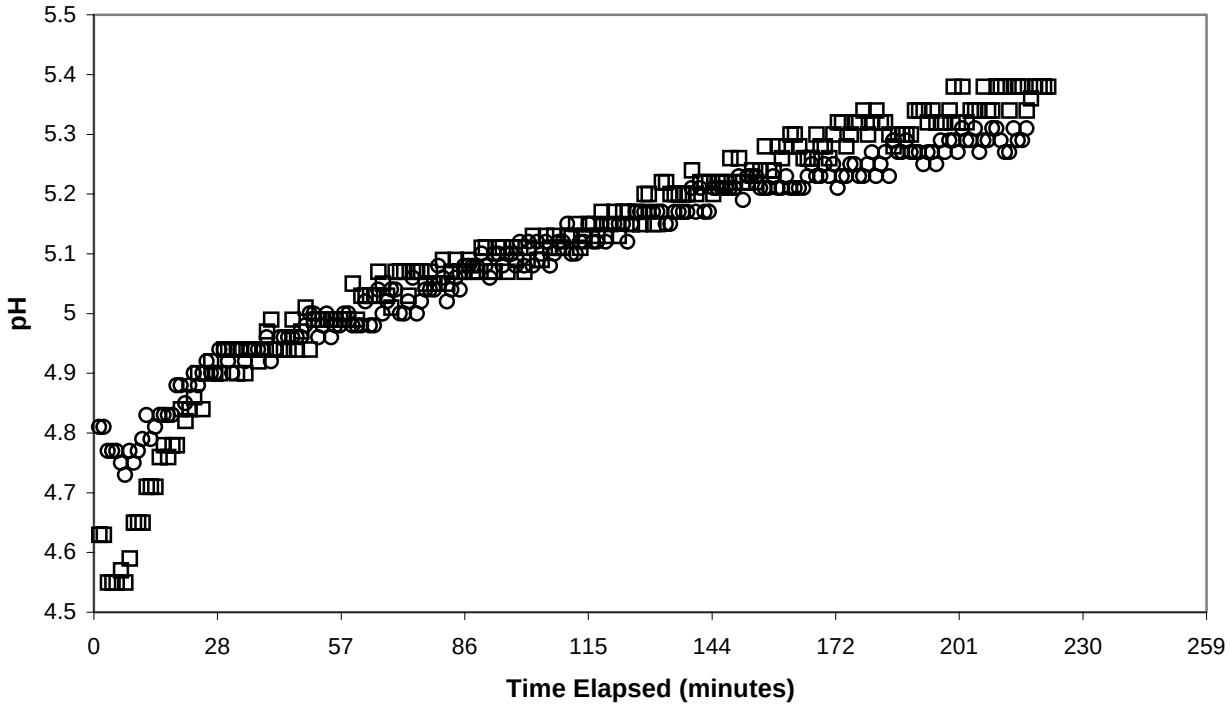

Fig. 5. Lead sorbed in the $NaNO_3$ matrix without any solid, mineral-blank in $NaNO_3$, versus pH. Filter paper is in the experiment by design even for blank experiments. The open symbols show the pH data over elapsed time of the duplicate runs.

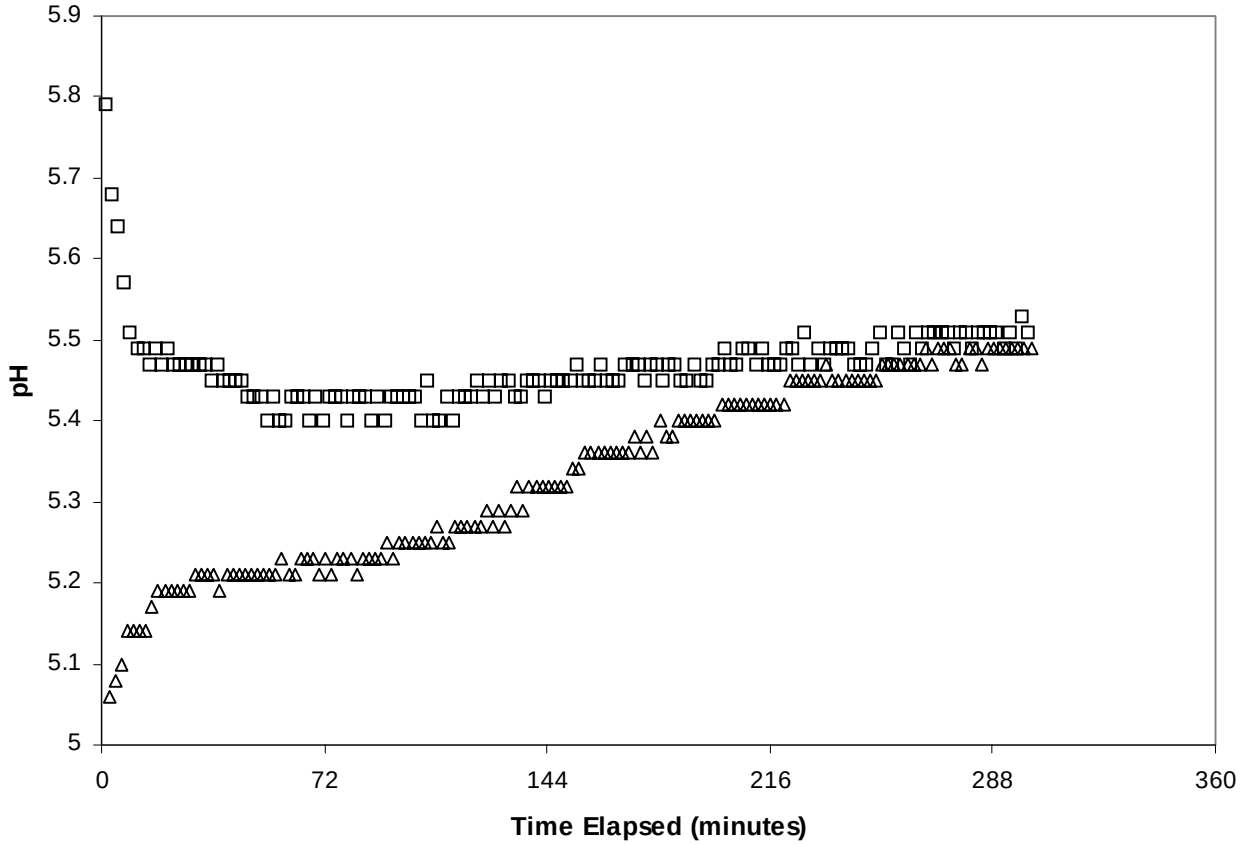

Fig. 6. Blank experiment without Pb or mineral solid in KNO_3 electrolyte, mineral-Pb-blank in KNO_3. The chosen filter paper was used in the blanks. The open symbols show the pH of the effluent solution over time of duplicate runs.

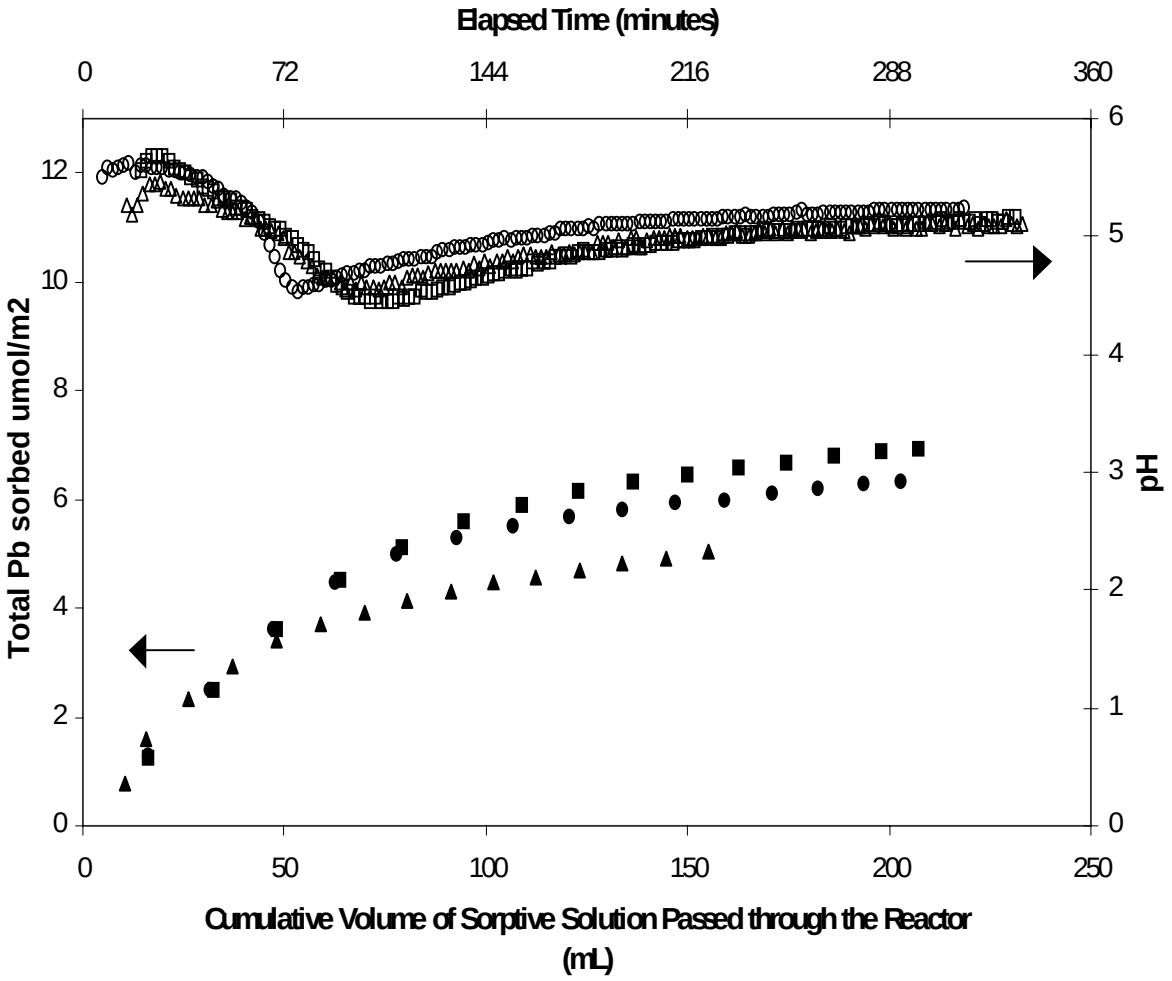

Fig. 7. Lead sorbed on synthetic cryptomelane in $NaNO_3$ background electrolyte and reaction pH. The reaction pH is plotted versus elapsed time using open symbols, and the Pb sorption is plotted in terms of the total amount of Pb sorbed normalized to the surface area of the solid using closed symbols. The plot shows triplicate runs.

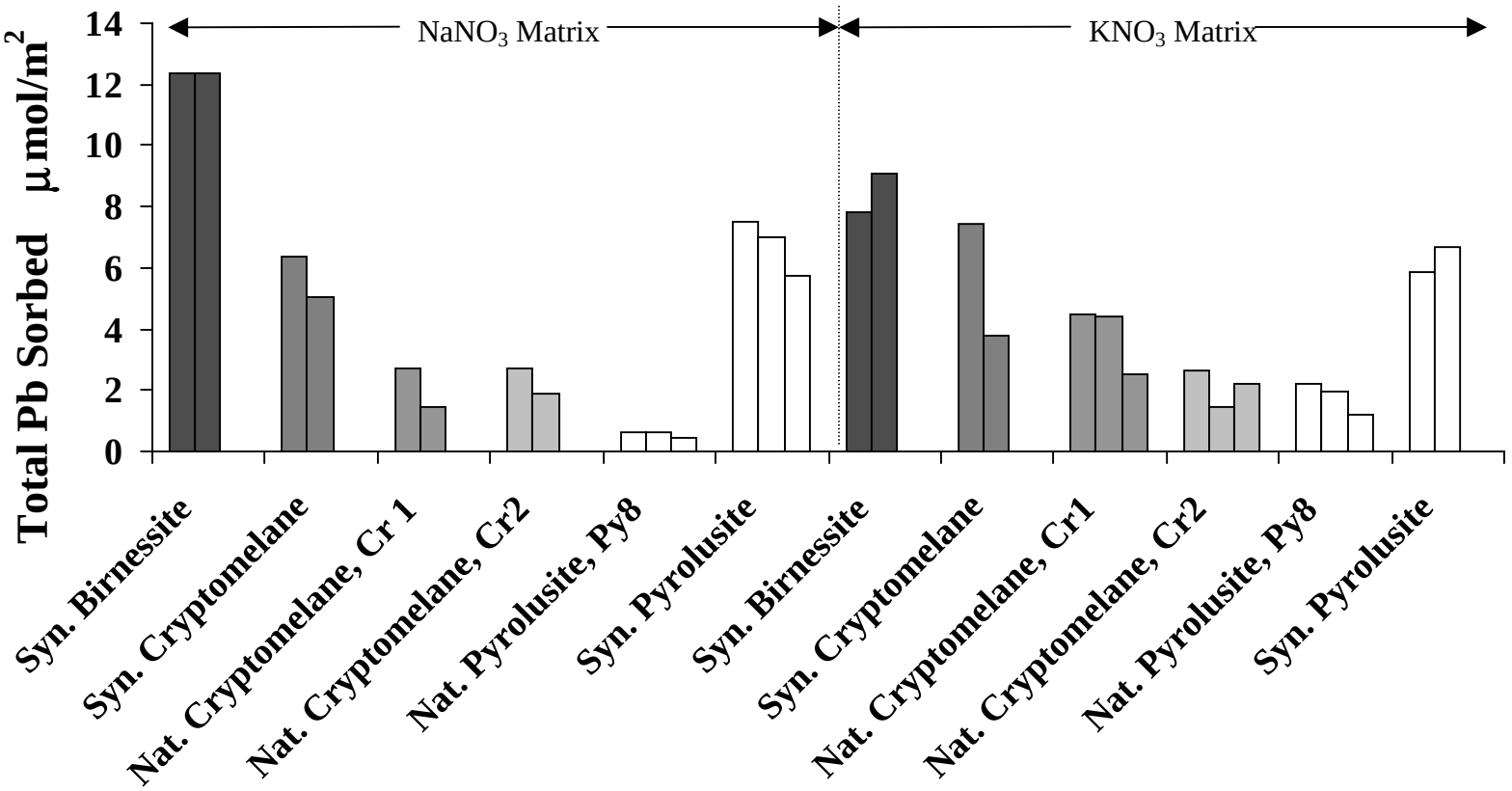

Fig. 8. Total Pb sorption on Mn-oxides displayed normalized to the BET surface area of the respective solid. All replicates used to generate the mean and the standard error of the mean are shown. Experiments run in $NaNO_3$ background electrolyte are shown on the left and experiments run in KNO_3 electrolyte are shown on the right.

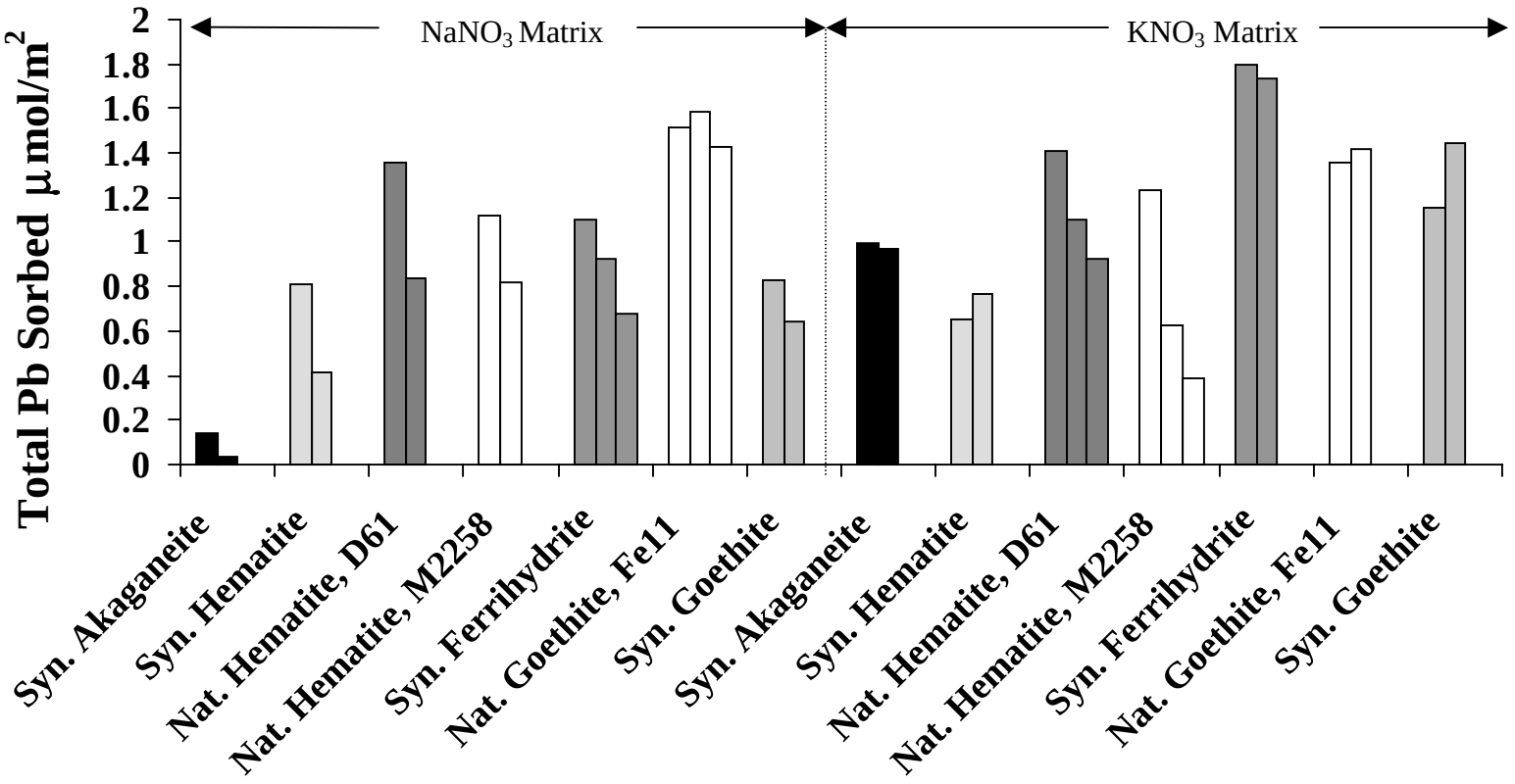

Fig. 9. Total Pb sorption on Fe-oxides displayed normalized to the BET surface area of the respective solid. All replicates used to generate the mean of the standard error of the meanare shown. Experiments run in $NaNO_3$ background electrolyte are shown on the left and experiments run in KNO_3 electrolyte are shown on the right.

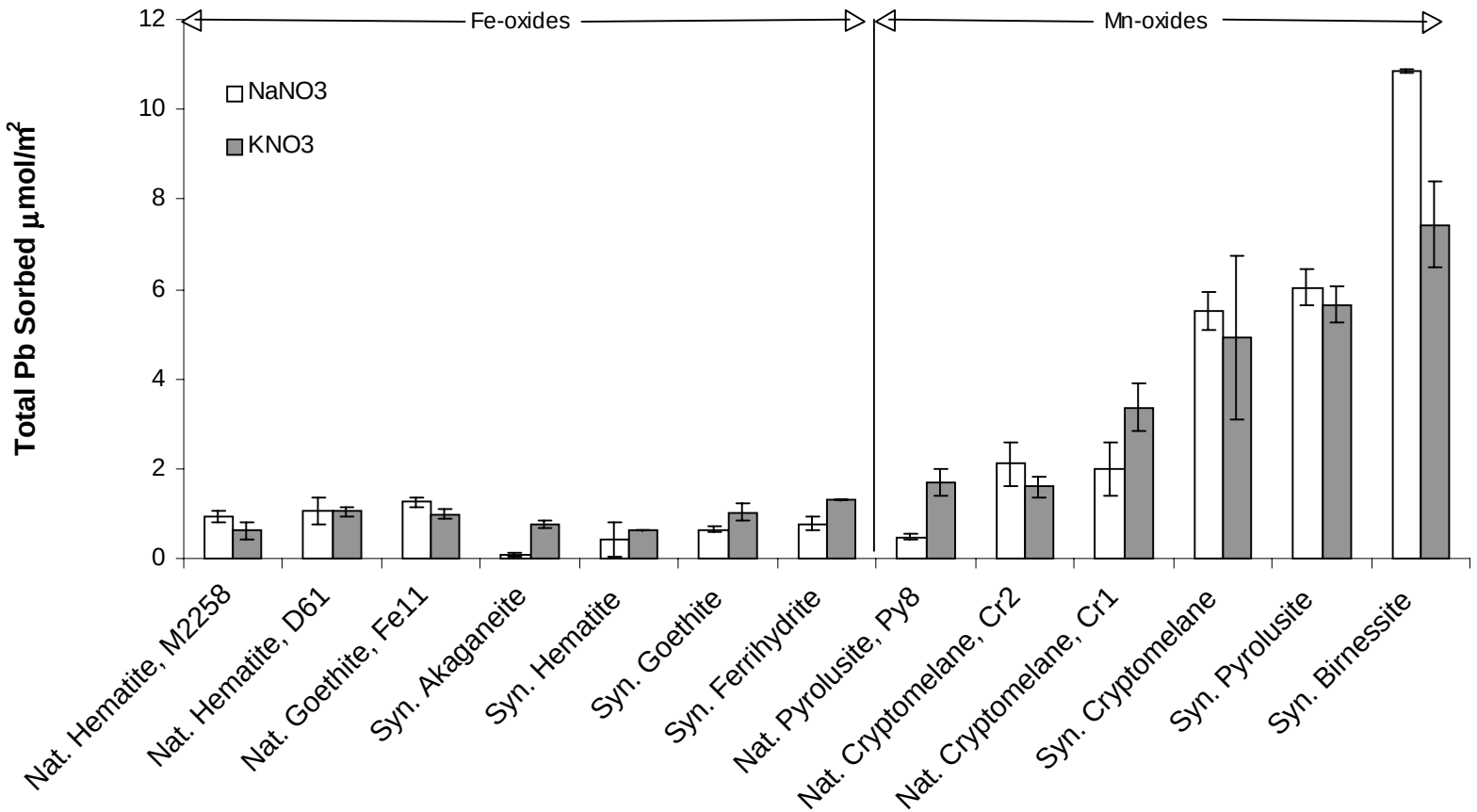

Fig. 10. Total average Pb sorption in umol/m^2 (normalized to the BET surface area of the solid) after approximately 118mL of solution has passed through each reactor. The error bars denote plus or minus the standard error of the mean. Studies conducted in $NaNO_3$ background electrolyte are displayed using white bars while studies conducted in KNO_3 background electrolyte are denoted by gray bars. The Fe-oxides are listed to the left, and the Mn-oxides are listed on the right of the figure.

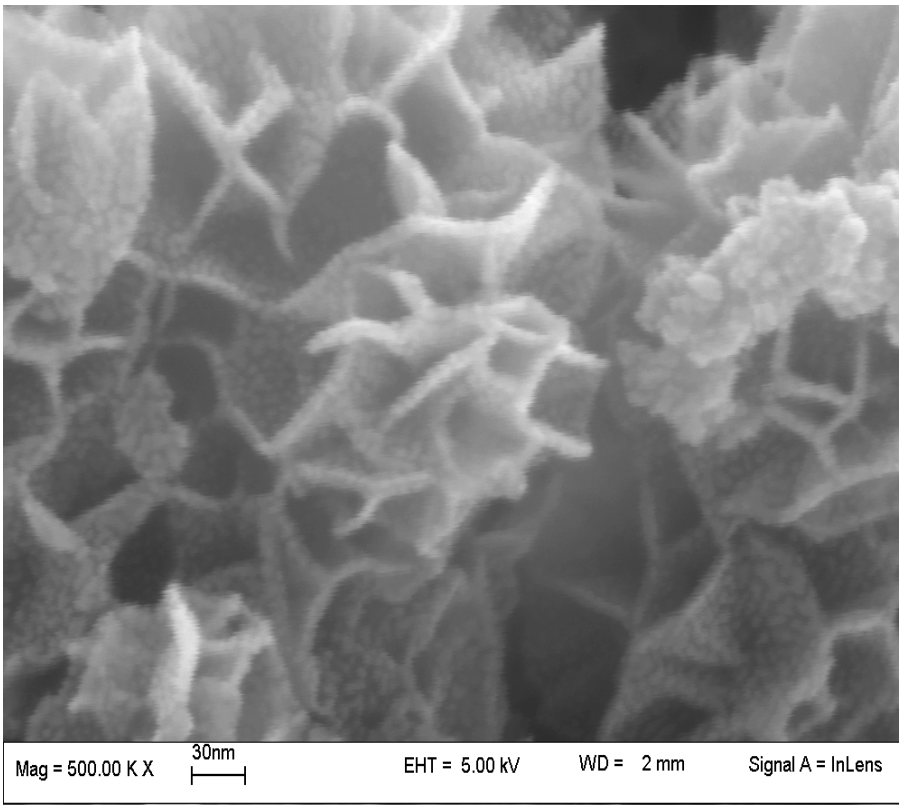

Fig. 11. FE-SEM image of synthetic birnessite. The scale bar denotes 30 nm. The image shows that the morphology is similar to that of a baerite rose. The minute bumps on the plate surfaces are due to the gold conductive coating applied to the unreacted sample before SEM imaging.

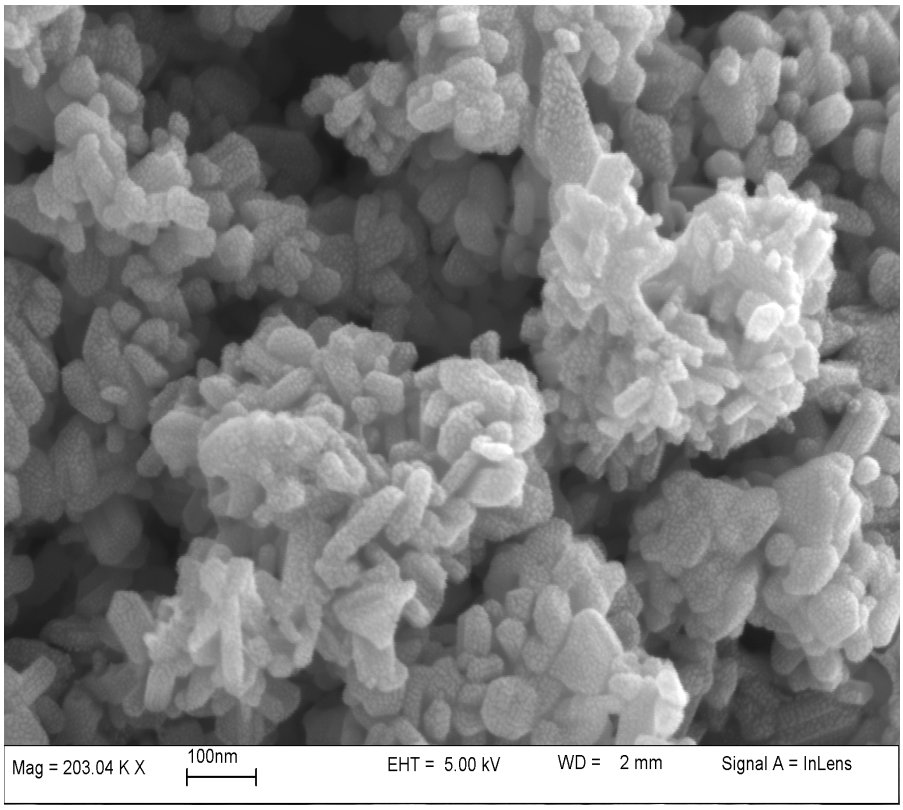

Fig. 12. FE-SEM image of synthetic cryptomelane. Note the scale bar denotes 100 nm. The image shows that the crystal morphology is dominated by hexagonal platelets; the minute bumps on the plate surfaces are due to the gold conductive coating applied to the unreacted sample before SEM imaging.

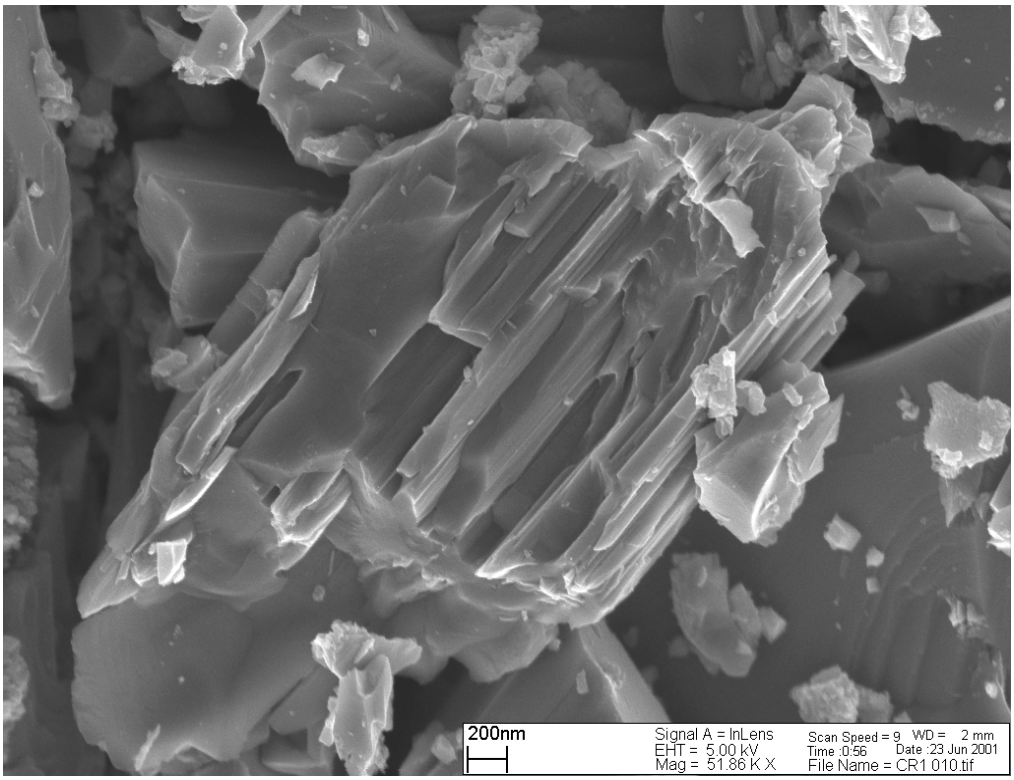

Fig. 13. FE-SEM image of natural cryptomelane, Cr1 without any conductive coating. Note the scale bar denotes 200 nm.

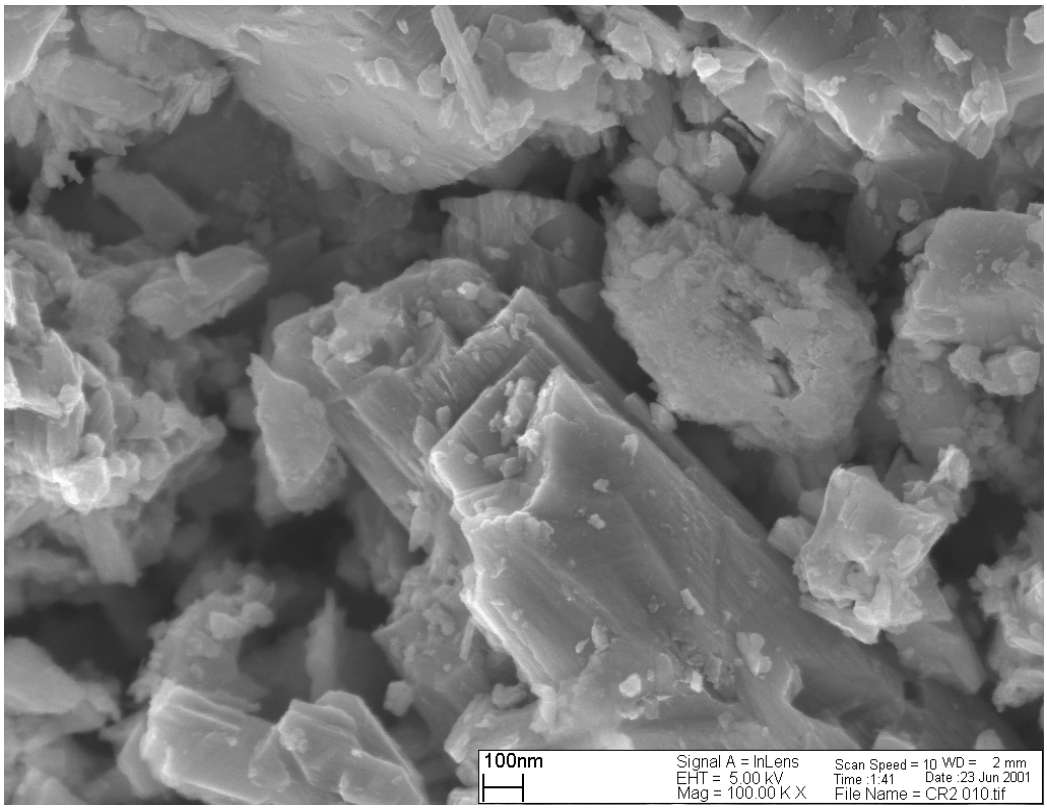

Fig. 14. FE-SEM image of natural cryptomelane, Cr2 without any conductive coating. The scale bar denotes 100 nm.

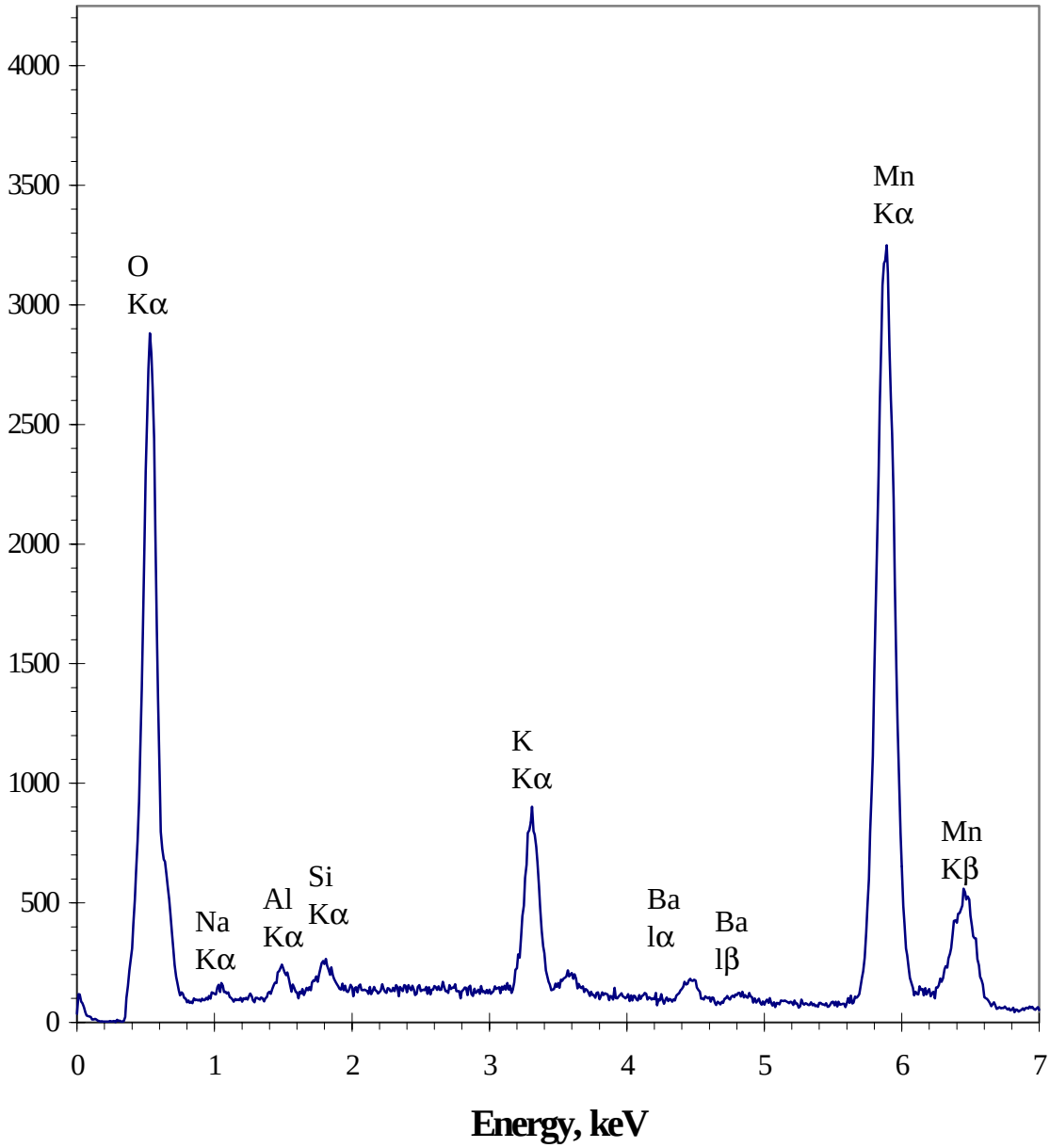

Fig. 15. EDS spectra of unreacted natural cryptomelane, Cr1.

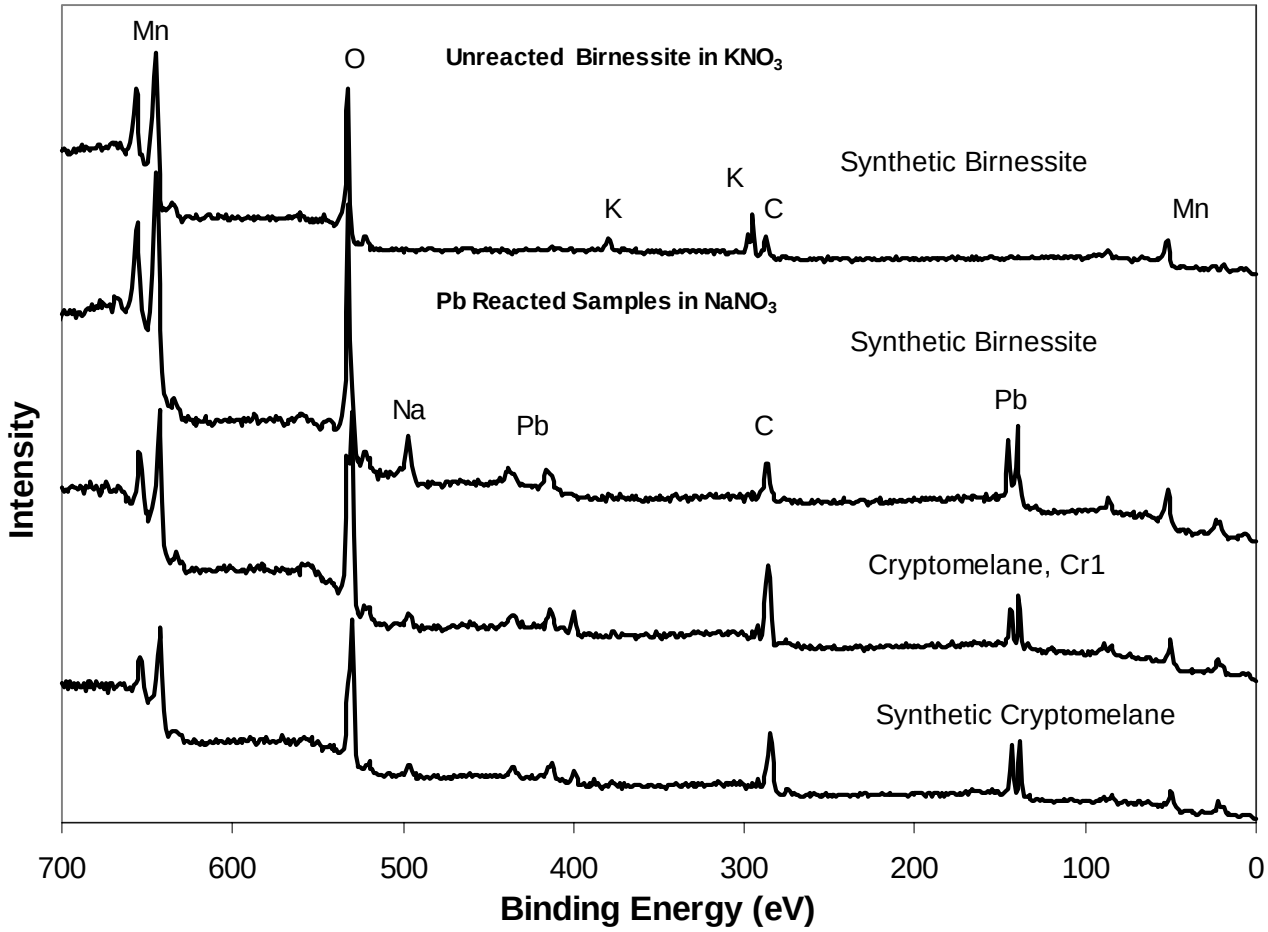

Fig. 16. XPS survey scans of unreacted synthetic birnessite in KNO_3 and selected Pb reacted samples in $NaNO_3$ background electrolyte. The major peaks have been identified.

8 VITA

SUSAN ERIN O'REILLY

Department of Geological Sciences •Virginia Polytechnic Institute and State University,
Blacksburg, VA 24061 •

EDUCATION

Virginia Polytechnic Institute and State University
Ph.D., 10/02
Dissertation: Lead Sorption Efficiencies of Mn and Fe-oxides
University of Delaware
MS, 7/98
Thesis: Arsenate sorption/desorption kinetics and competition reactions on goethite

University of Delaware
BS, 5/96
Major: *Environmental Soil Science*
Minor: *Chemistry*
Honors: *Magna Cum Laude*
Degree with Distinction

UNIVERSITY OF GEORGIA
BS, Environmental Soil Science, Attended from 9/92 to 6/93.

EMPLOYMENT

VIRGINIA POLYTECHNIC INSTITUTE AND STATE UNIVERSITY
Graduate Research Assistant, 5/99-present
Graduate Teaching Assistant, 8/98-5/99
Advisor: Dr. M.F. Hochella, Jr.

- Taught introductory geology lab for engineers (3 sections, 25 students)
- Synthesized Mn and Fe oxides; collected and prepared natural oxides
- Characterized samples using XRD, FE-SEM, and N_2-BET
- Designed a flow reactor system with computerized pH monitoring capabilities
- Analyzed Pb wet chemical data using AA and Excel
- Examined reacted solids with FE-SEM, XPS
- Wrote a research proposal
- Spoke at professional meetings

UNIVERSITY OF DELAWARE
Graduate Research Fellow, 7/96 – 7/98
Environmental Soil Chemistry Laboratory
Advisor: Dr. D.L. Sparks.

Synthesized goethite
Conducted pH-stat batch adsorption and desorption studies
Analyzed As samples via ICP-AES
Analyzed reacted solids with EXAFS
Developed batch competition studies with other anions
Spoke at professional meetings and published the research

DUPONT AGRICULTURAL PRODUCTS
Intern, 5/95 - 8/95
Advisor: Dr. Larry Tapia.
Managed data in Excel and helped develop Power Point presentations for the Soybean Herbicide Division

SCIENCE AND ENGINEERING RESEARCH SEMESTER SPONSORED BY THE DEPARTMENT OF ENERGY
Intern, 1/95 - 5/95
Advisor: Dr. A.J. Stewart
Researched the phytotoxicity of lithium using *Arabidopsis*

DUPONT (THROUGH A CONTRACT WITH NORELL SERVICES)
Laboratory Assistant, 6/94 - 8/94
Phytoremediation Laboratory
Advisors: Dr. Scott Cunningham and Dr. Bill Berti.
Tested Pb bioavailability through innovative laboratory methods

UNIVERSITY OF DELAWARE
Laboratory Assistant, 6/93 - 5/94
Soil Chemistry Laboratory
Advisor: Dr. D.L. Sparks.

UNIVERSITY OF DELAWARE
Laboratory Assistant, 6/93 - 9/93
Soil Fertility Laboratory
Advisor: Dr. J.T. Sims.

UNIVERSITY OF GEORGIA
Laboratory Assistant, 9/92 - 6/93
Soil Fertility Laboratory
Advisor: Dr. M.E. Sumner.

RESEARCH PRESENTATIONS

"PB SORPTION EFFICIENCIES ON NATURAL AND SYNTHETIC MN AND FE-OXIDES: A NEW LOOK AT AN OLD PROBLEM" AT THE 2002 ACS NATIONAL MEETINGS, ORLANDO, FL. ADVISOR: DR. M.F. HOCHELLA, JR.

"New Approaches to the Study of Lead Sorption Efficiencies on Natural and Synthetic Mn and Fe-Oxides" AT THE 2001 SSSA ANNUAL MEETINGS, CHARLOTTE, NC. Advisor: Dr. M.F. Hochella, Jr.

POSTER "Competitive Effects of Phosphate and Sulfate on Kinetics of Arsenate Sorption on Goethite" AT THE 1998 SSSA ANNUAL MEETINGS, BALTIMORE, MD. Advisor: Dr. D.L. Sparks.

"The Effects of Residence Time on Arsenate Sorption/Desorption by Goethite" AT THE 1997 SSSA ANNUAL MEETINGS, ANAHEIM, CA. Advisor: Dr. D.L. Sparks.

POSTER "The Effects of Residence Time on the Retention of Arsenate by Goethite" AT THE 1997 ACS DIVISION OF GEOCHEMISTRY MEETINGS, SAN FRANCISCO, CA. Advisor: Dr. D.L. Sparks.

DEGREE WITH DISTINCTION "The Effects of Residence Time on the Retention of Arsenate by Goethite" AT THE 1996 UNDERGRADUATE RESEARCH SYMPOSIUM AT THE UNIVERSITY OF DELAWARE. Advisor: Dr. D.L. Sparks.

"Assessing the phytotoxicity of lithium using *Arabidopsis"* AT THE SPRING 1995 SCIENCE AND ENGINEERING RESEARCH SEMESTER SYMPOSIUM. Advisor: Dr. A. J. Stewart.

"Phosphorus Sorption and Desorption in Soils Amended with Coal Fly Ash" AT THE 1994 ANNUAL MEETING OF THE NORTHEASTERN BRANCH OF THE AMERICAN SOCIETY OF AGRONOMY. Advisor: Dr. J. T. Sims.

REFEREED PUBLICATIONS TO DATE

O'REILLY, S.E., D.G STRAWN, AND D.L. SPARKS. 2001. RESIDENCE TIME EFFECTS ON ARSENATE ADSORPTION/DESORPTION MECHANISMS ON GOETHITE. SOIL SCI. SOC. AM. J. 65:67-77.

O'REILLY, S.E., AND J.T. SIMS. 1995. PHOSPHORUS ADSORPTION AND DESORPTION IN A SANDY SOIL AMENDED WITH HIGH RATES OF COAL FLY ASH. COMMUN. SOIL SCI. PLANT ANAL. 26(17&18):2983-2993.

ADDITIONAL PAPERS IN PREPARATION

PROFESSIONAL SOCIETIES

AMERICAN CHEMICAL SOCIETY
CLAY MINERALS SOCIETY
GEOCHEMICAL SOCIETY
MINERALOGICAL SOCIETY OF AMERICA
SOIL SCIENCE SOCIETY OF AMERICA

AWARDS & HONORS

5/1999-PRESENT	NSF RESEARCH STIPEND, PROJECT TITLE: MINERAL-WATER INTERFACE DYNAMICS: THE COMPLEX INTERACTIONS OF REDOX ACTIVE METALS WITH MANGANESE OXIDE SURFACES
1996-1998	GRADUATE RESEARCH FELLOWSHIP, COLLEGE OF AGRICULTURAL SCIENCES, UNIVERSITY OF DELAWARE.
1996	SENIOR STUDENT AWARD FROM THE NORTHEASTERN BRANCH OF THE AMERICAN SOCIETY OF AGRONOMY.
1996	PANEL OF SCHOLARS BY MAJOR, ENVIRONMENTAL SOIL SCIENCE, COLLEGE OF AGRICULTURE, UNIVERSITY OF DELAWARE.
1994-PRESENT	MEMBER OF THE GOLDEN KEY NATIONAL HONOR SOCIETY.
1994-96	DELAWARE-MARYLAND AGRIBUSINESS ASSOCIATION SCHOLARSHIP.
1994-96	AGRICULTURAL AMBASSADOR (REPRESENTATIVE OF THE COLLEGE OF AGRICULTURAL SCIENCES, UNIVERSITY OF DELAWARE).
1994-95	ENVIRONMENTAL SOIL SCIENCE FACULTY AWARD.
1993-96	CARAVEL AGRICULTURAL SCHOLARSHIP.
1992-96	DEAN'S LIST.
1992-93	Frederick B. & Marjorie W. Smith Scholarship in Soil Science, University of Georgia.